

Model for $q^2\bar{q}^2$ systems, illustrated by an application to $K\bar{K}$ scattering

B. Masud*

Research Institute for Theoretical Physics, P.O.Box 9, SF-00014, University of Helsinki, Finland

(Received 14 January 1994)

Presented here is a lattice-gauge-theory-motivated four-body potential model for $q^2\bar{q}^2$ systems which includes both the spin and flavor degrees of freedom, extending the formalism presented already in the spin-independent situation. This allows an application to a realistic situation, which is chosen to be $K\bar{K}$ scattering. It is seen that because of the gluonic effects in this multiquark system, the $K\bar{K}$ attraction resulting from the quark-exchange mechanism gets appreciably decreased compared to that emerging through the naive two-body potential approach.

PACS number(s): 13.75.Lb, 12.38.Lg, 12.39.Pn, 14.40.Aq

I. INTRODUCTION

With strong evidence in favor of quark confinement both from experiment (failure to find free quarks) and theory [1,2], we have some understanding of the quark-quark interaction for large distances. Combining this with the understanding of the short distance quark-quark interaction obtained through perturbative QCD, different models of the quark-quark interaction have been used such as the MIT bag model [3,4] and the constituent quark potential model. In the constituent quark potential model the quark-antiquark interaction is represented by a potential which is given by the one-gluon exchange mechanism, but is modified so as to incorporate the confining potential as the limit for large distances. Moreover, the current masses of the QCD Lagrangian are replaced by effective masses, termed *constituent masses*, which are fitted to experimentally known quantities. For quarks of known (fitted) masses interacting through a space-dependent potential, one can set up and solve a Schrödinger equation for their dynamics. In this way the constituent quark potential model explains in a consistent and unified way most of the observed mesonic states as quark-antiquark states with different values of orbital and radial quantum numbers [5].

But that is not enough. A successful model of strong interactions should be able to describe also possible systems having three or more quarks and/or antiquarks. It is not clear yet how, if at all, the quark potential model can be applied to multiquark systems. Perhaps the simplest approach is to take the many-body Hamiltonian as a sum of Hamiltonians corresponding to all pairs of particles involved, the basic method used in [6–9]. But this has many theoretical as well as phenomenological (such as the van der Waals force problem [10]) flaws. Keeping this in mind, a *four-body* potential model for a quark-exchange mechanism in $q^2\bar{q}^2$ systems was proposed in [11]

in a spin-independent situation. This model takes into account the effects of the gluonic degrees of freedom in a nontrivial way. Only for small distances does this agree with the sum of two-body ($\mathbf{F}_i \cdot \mathbf{F}_j$) potentials model. For interquark distances greater than, roughly speaking, 0.5 fm it qualitatively agrees with the flux tube model [12,13] of the gluonic field.

In the present paper this model is extended to the realistic situation of spin and flavor dependence. These new degrees of freedom are introduced in Sec. III, after a brief review of the already published model of the gluonic field in Sec. II. Then as a first application the model is applied to a physical meson-meson system, namely, $K\bar{K}$, in Sec. IV. The solution for the total wave function of the system thus obtained gives us a condition for the existence of a bound state of the whole system, along with numerical results for corresponding phase shifts. All this is reported in Sec. V, followed by our conclusions in Sec. VI.

II. THE MODEL OF THE GLUONIC FIELD

As shown in [12], there are three independent flux tube topologies for the gluonic field of the $N_q = N_{\bar{q}} = 2$ system. Two of them [shown as (a) and (b) in Fig. 1] are extensions of the usual *two-dimensional* color basis [7] used in the two-body model. The third state [shown as (c) in Fig. 1] arises through a generalization of the three-gluon-type mechanism in QCD. The gluonic field in this state would be similar to that in a baryonium (or in an interacting baryon-antibaryon pair with a quark-antiquark pair removed). The introduction of this state may be the first (though not essential) step towards incorporation of the gluonic effects in $q^2\bar{q}^2$ systems. Thus needing a basis containing at least *three* gluonic states for a good description of the corresponding gluonic field, a convenient starting point for constructing a model for these sorts of systems would be to write the two-body potential model for them in a redundant color basis:

*Present address: Department of Physics, Punjab University, Lahore, Pakistan.

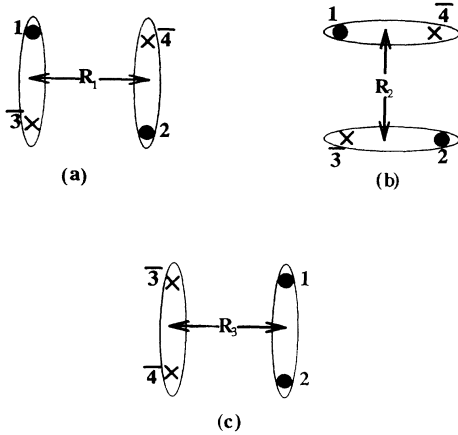


FIG. 1. Three different topologies of the diquark-diantiquark system.

$$|1\rangle_c = |1_{1\bar{3}}1_{2\bar{4}}\rangle_c, |2\rangle_c = |1_{1\bar{4}}1_{2\bar{3}}\rangle_c,$$

and (2.1)

$$|3\rangle_c = |\bar{3}_{12}\bar{3}_{\bar{3}\bar{4}}\rangle_c.$$

These correspond to the three basic states in the flux tube model. The two-body potential model Hamiltonian written in this redundant basis will have the usual con-

finement, kinetic energy, and other (such as hyperfine) parts. For the confinement term we take (as in [11])

$$V^{cf} = \sum_{i<j} \mathbf{F}_i \cdot \mathbf{F}_j v_{ij}, \quad (2.2)$$

with

$$v_{ij} = Cr_{ij}^2 + \bar{C}. \quad (2.3)$$

This quadratic form of the two-body potential is used basically for computational convenience. It has been used frequently in quark descriptions of NN scattering [14,15] and also in pseudoscalar meson-meson scattering [16]. Similarly, for the kinetic energy part, the nonrelativistic expression is used.

By simple calculations of color overlap factors, the overlap matrix N in the above mentioned basis is obtained as

$$N = \begin{pmatrix} 1 & \frac{1}{3} & \sqrt{\frac{1}{3}} \\ \frac{1}{3} & 1 & -\sqrt{\frac{1}{3}} \\ \sqrt{\frac{1}{3}} & -\sqrt{\frac{1}{3}} & 1 \end{pmatrix}. \quad (2.4)$$

For the potential matrix, one has to calculate matrix elements of the $\mathbf{F}_i \cdot \mathbf{F}_j$ (or $\lambda \cdot \lambda$) operator. This can be simplified by using the results of Appendix C of [7]. The result is

$$V^{cf} = \begin{pmatrix} -\frac{4}{3}(v_{1\bar{3}} + v_{2\bar{4}}) & \frac{4}{9} \begin{pmatrix} v_{12} + v_{\bar{3}\bar{4}} \\ -v_{1\bar{3}} - v_{2\bar{4}} \\ -v_{1\bar{4}} - v_{2\bar{3}} \end{pmatrix} & \frac{2}{3\sqrt{3}} \begin{pmatrix} -2(v_{1\bar{3}} + v_{2\bar{4}}) \\ +v_{1\bar{4}} + v_{2\bar{3}} \\ -v_{12} - v_{\bar{3}\bar{4}} \end{pmatrix} \\ -\frac{4}{3}(v_{1\bar{4}} + v_{2\bar{3}}) & \frac{2}{3\sqrt{3}} \begin{pmatrix} 2(v_{1\bar{4}} + v_{2\bar{3}}) \\ +v_{12} + v_{\bar{3}\bar{4}} \\ -v_{2\bar{4}} - v_{1\bar{3}} \end{pmatrix} \\ \text{symmetric} & -\frac{1}{3} \begin{pmatrix} 2(v_{12} + v_{\bar{3}\bar{4}}) \\ +v_{1\bar{3}} + v_{2\bar{4}} \\ +v_{1\bar{4}} + v_{2\bar{3}} \end{pmatrix} \end{pmatrix}. \quad (2.5)$$

The matrix element of the nonrelativistic kinetic energy operator between any two color states is simply taken to be proportional to their overlap: i.e.,

$${}_c\langle X'|K|X\rangle_c = \sum_i -\frac{\nabla_i^2}{2m_i} {}_c\langle X'|X\rangle_c. \quad (2.6)$$

More gluonic effects in $q^2\bar{q}^2$ systems can be included by multiplying the *off-diagonal* elements in the above matrices (or even in the corresponding truncated 2×2 matrices) by a space-dependent factor. This treatment of the off-diagonal elements of the two-body-model-based matrices is motivated by the work presented in [17,18], which show that in the flux tube model the coupling of the three gluonic states $|1\rangle_g$, $|2\rangle_g$, and $|3\rangle_g$ [corresponding to the three-dimensional color basis defined in Eq. (2.1)] decreases exponentially with interquark distances.

Moreover, we note that for large interquark distances the space-dependence of the diagonal elements of the K , V^{cf} , and N matrices in both the two-body potential and the flux tube model are similar, and use this form for all distances, i.e., do not alter the diagonal elements in the above matrices. For the space-dependent factor f multiplying the off-diagonal elements, the choice used in [11] was

$$f = \exp\left(-\bar{k} \sum_{i<j} r_{ij}^2\right), \quad \bar{k} = \frac{1}{6}kb_s, \quad (2.7)$$

with k a numerical coefficient. This is the simplest choice from a computational point of view. An alternative choice of f is suggested here to be

$$f = \exp(-b_s E \mathcal{A}), \quad (2.8)$$

with E a numerical constant, and \mathcal{A} the area bounded by the four outer lines connecting the four particles 1, 2, $\bar{3}$, and $\bar{4}$:

$$\mathcal{A} = \int_0^1 \int_0^1 dx dy \left| [x\mathbf{r}_{1\bar{3}} + (1-x)\mathbf{r}_{4\bar{2}}] \times [y\mathbf{r}_{2\bar{3}} + (1-y)\mathbf{r}_{4\bar{1}}] \right|. \quad (2.9)$$

For planar geometries this becomes what is proposed in [19,20]. Both of these forms have been studied in [21–23], which aim at extracting the gluon field overlap factor f from a calculation using lattice Monte Carlo techniques. This work is in progress and so far no definite conclusions have been arrived at. For the dynamical calculations

done in the present work, we have used the simpler sum-of-squares form [Eq. (2.7)].

The resulting expressions are used in this work as matrix elements of the overlap, kinetic, and potential energy operators. These are, respectively,

$$N(f) = \begin{pmatrix} 1 & \frac{1}{3}f & \sqrt{\frac{1}{3}}f \\ \frac{1}{3}f & 1 & -\sqrt{\frac{1}{3}}f \\ \sqrt{\frac{1}{3}}f & -\sqrt{\frac{1}{3}}f & 1 \end{pmatrix}, \quad (2.10)$$

$$K(f)_{X',X} = N(f)_{X',X}^{1/2} \left(\sum_i -\frac{\nabla_i^2}{2m_i} \right) N(f)_{X',X}^{1/2}, \quad (2.11)$$

and

$$V^{cf}(f) = \begin{pmatrix} -\frac{4}{3}(v_{1\bar{3}} + v_{2\bar{4}}) & \frac{4f}{9} \begin{pmatrix} v_{12} + v_{\bar{3}\bar{4}} \\ -v_{1\bar{3}} - v_{2\bar{4}} \\ -v_{1\bar{4}} - v_{2\bar{3}} \end{pmatrix} & \frac{2f}{3\sqrt{3}} \begin{pmatrix} -2(v_{1\bar{3}} + v_{2\bar{4}}) \\ +v_{1\bar{4}} + v_{2\bar{3}} \\ -v_{12} - v_{\bar{3}\bar{4}} \end{pmatrix} \\ & -\frac{4}{3}(v_{1\bar{4}} + v_{2\bar{3}}) & \frac{2f}{3\sqrt{3}} \begin{pmatrix} 2(v_{1\bar{4}} + v_{2\bar{3}}) \\ +v_{12} + v_{\bar{3}\bar{4}} \\ -v_{2\bar{4}} - v_{1\bar{3}} \end{pmatrix} \\ \text{symmetric} & & -\frac{1}{3} \begin{pmatrix} 2(v_{12} + v_{\bar{3}\bar{4}}) \\ +v_{1\bar{3}} + v_{2\bar{4}} \\ +v_{1\bar{4}} + v_{2\bar{3}} \end{pmatrix} \\ & & +\frac{5}{2}Df(1-f) \end{pmatrix}. \quad (2.12)$$

The basis now is actually $|1\rangle_g, |2\rangle_g$, and $|3\rangle_g$, instead of $|1\rangle_c, |2\rangle_c$, and $|3\rangle_c$; the new subscript g refers to the gluonic degree of freedom. Introduction of the additional $\frac{5}{2}Df(1-f)$ term even in a diagonal (3,3) element of the proposed potential matrix [Eq. (2.12)] guarantees that our gluonic basis does *not* reduce for vanishing distances to a redundant basis. Actually the third base state is $D \approx 1.5$ GeV higher than the other two for small distances. See [11] [from Eq. (4.18) to the end of Sec. IV] for details.

III. THE SPIN AND FLAVOR DEPENDENCE

For the spin-dependent part of the basis we use states arising through spin of the quarks only, and, being interested in the ground state of the $J^P = 0^+$ sector of the system, we focus on spin states with the total spin of the system as zero. In each of the three channels corresponding to the three gluonic states $|1\rangle_g, |2\rangle_g$, and $|3\rangle_g$, the four particles can be grouped into two mesonic subclusters. Each of these mesonic clusters may have a spin of zero or 1 and hence the $q^2\bar{q}^2$ system may be composed of either two spin singlets or two triplets, meaning that there may be *two* independent spin channels for each of the three gluonic channels above. Thus, there are *six* independent states of the system in hand. The corre-

sponding six spin states are written in the notation of Appendix D of [7] (see Appendix A of the present paper for details) as follows.

In the first channel (with the gluonic part of the base states for both spin configurations as $|1\rangle_g$),

$$|1S\rangle_s = |P_{1\bar{3}}P_{2\bar{4}}\rangle_s \quad \text{and} \quad |1T\rangle_s = |\mathbf{V}_{1\bar{3}} \cdot \mathbf{V}_{2\bar{4}}\rangle_s. \quad (3.1)$$

In the second channel,

$$|2S\rangle_s = |P_{1\bar{4}}P_{2\bar{3}}\rangle_s \quad \text{and} \quad |2T\rangle_s = |\mathbf{V}_{1\bar{4}} \cdot \mathbf{V}_{2\bar{3}}\rangle_s. \quad (3.2)$$

In the third channel,

$$|3S\rangle_s = |S_{12}S_{\bar{3}\bar{4}}\rangle_s \quad \text{and} \quad |3T\rangle_s = |\mathbf{A}_{12} \cdot \mathbf{A}_{\bar{3}\bar{4}}\rangle_s. \quad (3.3)$$

In this notation S_{ij} and \mathbf{A}_{ij} stand for the scalar and axial vector spin wave functions, respectively, and the pseudoscalar and vector spin wave functions P_{ij} and \mathbf{V}_{ij} are defined in terms of their linear combinations.

For writing down the spin-dependent part of the Hamiltonian we proceed as in the last section: first consider the Hamiltonian in the two-body potential model limit and then multiply the off-diagonal elements by the space-dependent function f . The spin-dependent part of the Hamiltonian would be composed of the terms corresponding to hyperfine (contact as well as tensor) and

spin-orbit interactions, but because of our constraint to the S -wave ground states, only the hyperfine contact interaction has to be considered. For the hyperfine term in the two-body potential model limit we take the expression (used, with some modifications, in [7]) given by one-gluon exchange and summed over all the pairs:

$$V^{\text{hyp}} = \sum_{i<j} V_{ij}^{\text{hyp}} = - \sum_{i<j} \mathbf{F}_i \cdot \mathbf{F}_j \frac{8\pi\alpha_s^{ij}}{3m_i m_j} \delta^3(\mathbf{r}_{ij}) \mathbf{S}_i \cdot \mathbf{S}_j. \quad (3.4)$$

The numerical values of α_s^{ij} will be taken in this work as varying with the sum of the masses of the particles i and j ; thus each of them will eventually be replaced by α_s^l , α_s^{ls} , or α_s^{ss} , l standing for a quark(antiquark) of light mass and s for a strange one.

In the present paper the flavor dependence is mostly taken to be trivial, just giving rise to isospin-conserving factors. Actually, flavor changing is possible in any channel through pair annihilation of quarks and antiquarks of the same flavor, but we incorporate this *only* in the diagonal term corresponding to the pseudoscalar-pseudoscalar sector of the second gluonic channel (see the next section). Here the pair annihilation and creation effects are represented by a Hamiltonian term V^a operating in the flavor space only. It is a sum of terms V_{ij}^a , one for every pair i and j of the same-flavor particles. The matrix elements of each V_{ij}^a are defined to be

$$\begin{aligned} {}_f\langle u\bar{u}|V_{ij}^a|u\bar{u}\rangle_f &= {}_f\langle d\bar{d}|V_{ij}^a|u\bar{u}\rangle_f = {}_f\langle d\bar{d}|V_{ij}^a|d\bar{d}\rangle_f = a_l, \\ {}_f\langle u\bar{u}|V_{ij}^a|s\bar{s}\rangle_f &= {}_f\langle d\bar{d}|V_{ij}^a|s\bar{s}\rangle_f = \sqrt{a_l}\sqrt{a_s} \end{aligned}$$

and

$${}_f\langle s\bar{s}|V_{ij}^a|s\bar{s}\rangle_f = a_s \quad (3.5)$$

in the corresponding flavor spaces. The mass (or flavor) dependence shown here is in qualitative agreement with that of the annihilation term H_A in [5]. In the above, a_l and a_s are phenomenological parameters to be fitted below to the masses and flavor wave functions of π , η , and η' mesons.

We now write down the Hamiltonian (for s waves only) of the $q^2\bar{q}^2$ systems, in a six-dimensional gluonic-spin basis [see Eqs. (3.1) – (3.3)], resulting from our model:

$$H = K(f) + V^{\text{cf}}(f) + V^{\text{hyp}}(f) + V^a + \sum_{i=1}^4 m_i. \quad (3.6)$$

Apart from a constant spin-overlap factor appearing in Eq. (A1), the X', X element of $K(f)$ is given by Eq. (2.11) and $V^{\text{cf}}(f)$ is [compare with Eq. (2.2)]

$$V^{\text{cf}}(f) = \sum_i \mathbf{F}_i \cdot \mathbf{F}_j(f) v_{ij}, \quad (3.7)$$

with v_{ij} given by Eq. (2.3); the $\mathbf{F}_i \cdot \mathbf{F}_j(f)$ operator is defined, in our three-dimensional gluonic basis, to be the same as the $\mathbf{F}_i \cdot \mathbf{F}_j$ operator resulting through the perturbative approach, except for multiplication of off-diagonal

elements by the f factor and addition of the $\frac{5}{2}Df(1-f)$ term in its (3,3) element [i.e., the modifications changing Eq. (2.5) to Eq. (2.12)]. $V^{\text{hyp}}(f)$ is [compare with Eq. (3.4)]

$$V^{\text{hyp}}(f) = - \sum_{i<j} \mathbf{F}_i \cdot \mathbf{F}_j(f) \frac{8\pi\alpha_s^{ij}}{3m_i m_j} \delta^3(\mathbf{r}_{ij}) \mathbf{S}_i \cdot \mathbf{S}_j, \quad (3.8)$$

and the annihilation part V^a is a sum of terms given by Eq. (3.5) above.

IV. $K\bar{K}$ SCATTERING

With quark contents of the $q^2\bar{q}^2$ system such as that of $K\bar{K}$, the flavor wave function can be written generally as $l\bar{s}l s$, l standing for u or d (actual combinations depending on isospin). We label these four particles $1, \bar{3}, \bar{4}$, and 2 , respectively. In this way the two same-flavor pairs in the $K\bar{K}$ systems are $1\bar{4}$ and $2\bar{3}$. Thus we will have

$$V^a = V_{1\bar{4}}^a + V_{2\bar{3}}^a, \quad (4.1)$$

with $V_{1\bar{4}}^a$ and $V_{2\bar{3}}^a$ given by Eq. (3.5). A look at Eq. (3.2) should now suffice to tell why the $2S$ channel is singled out for the incorporation of annihilation effects; here these effects are supposed to be responsible for the mass difference between (pseudoscalar) isoscalar and isovector mesons, i.e., η , η' , and π . The annihilation effects are negligible in the vector-vector sector of the second channel ($2T$ channel in our terminology), because of the small difference in the masses of the spin-1 isoscalar and isovector mesons ω and ρ .

With this labeling, the pair $(1, \bar{4})$ is composed of a light quark and a light antiquark, and $(2, \bar{3})$ of strange ones. Their mass ratio, equal to that of the strange quark mass m_s to the up (or down) quark mass m , is denoted by s in this paper. Antisymmetrization of the total wave function is not necessary in the present case since we do not have any two identical fermions.

So far no quark position dependence of the wave function has been talked about because of our adiabatic assumption (implicit in any potential model) that the slower quark motion can be studied separately under the influence of a potential simulating the “faster” motion of the gluonic field. Having written down a potential thus arising [see Eq. (3.6)], we can in principle write down and solve a Schrödinger equation for $K\bar{K}$ systems. But keeping in mind the complexity of the system (having nine degrees of freedom belonging to three independent vectors connecting four particles), we use an approximate method familiar in nuclear physics [24], and used now in particle physics as well [25]: the “resonating group method”. This corresponds to specifying parts of the quark position-dependent wave function before solving for the rest.

In the absence of annihilation effects, we can write down the total state vector of the whole system as a sum of six terms, each having the form of a quark position part, referred to as the “quark wave function” in the following, multiplied by a gluonic-spin base state.

This quark wave function is a function of four vectors $\mathbf{r}_1, \mathbf{r}_2, \mathbf{r}_3$, and \mathbf{r}_4 . These can be replaced by their combinations, with one of them as the center-of-mass coordinate of the whole system \mathbf{R}_c and three others which are taken here to be different in different channels. These are the following.

In the first channel (with the gluonic part of the wave function as $|1\rangle_g$),

$$\mathbf{R}_1 = \frac{\mathbf{r}_1 + s\mathbf{r}_3 - s\mathbf{r}_2 - \mathbf{r}_4}{1+s},$$

$$\mathbf{y}_1 = \mathbf{r}_1 - \mathbf{r}_3, \text{ and } \mathbf{z}_1 = \mathbf{r}_2 - \mathbf{r}_4. \quad (4.2)$$

In the second channel,

$$\mathbf{R}_2 = \frac{\mathbf{r}_1 + \mathbf{r}_4 - \mathbf{r}_2 - \mathbf{r}_3}{2},$$

$$\mathbf{y}_2 = \mathbf{r}_1 - \mathbf{r}_4, \text{ and } \mathbf{z}_2 = \mathbf{r}_2 - \mathbf{r}_3. \quad (4.3)$$

In the third channel,

$$\mathbf{R}_3 = \frac{\mathbf{r}_1 + s\mathbf{r}_2 - s\mathbf{r}_3 - \mathbf{r}_4}{1+s},$$

$$\mathbf{y}_3 = \mathbf{r}_1 - \mathbf{r}_2, \text{ and } \mathbf{z}_3 = \mathbf{r}_3 - \mathbf{r}_4. \quad (4.4)$$

$\mathbf{R}_1, \mathbf{R}_2$, and \mathbf{R}_3 are shown in Fig. 1. These are actually the vectors connecting the centers of masses of respective mesonic clusters. Other vectors in the above three equations connect particles inside the clusters.

In this paper the quark wave function in any channel is written as a product of two factors, one a function of \mathbf{R}_k and the other of \mathbf{y}_k and \mathbf{z}_k only, for $k = 1, 2$ or 3 . The former is denoted by $\chi_{kI}(\mathbf{R}_k)$, with I telling the spin state (singlet-singlet or triplet-triplet), and the latter by $\xi_k(\mathbf{y}_k)\zeta_k(\mathbf{z}_k)$. The spatial dependence of these on \mathbf{y}_k and \mathbf{z}_k is taken to be Gaussian in consistency with the choice of the quadratic form of the interquark potential in Eq. (2.3), but the χ_{kI} 's are treated as variational functions to be determined by solving the approximate coupled Schrödinger equations.

With these forms of the quark wave functions, the total state vector of the whole $q^2\bar{q}^2$ system is written as

$$|\Psi(q_1, q_2, \bar{q}_3, \bar{q}_4; g)\rangle = \sum_{kI} |k\rangle_g |kI\rangle_s |k\rangle_f \psi_c(\mathbf{R}_c)$$

$$\times \chi_{kI}(\mathbf{R}_k) \xi_k(\mathbf{y}_k) \zeta_k(\mathbf{z}_k), \quad (4.5)$$

with

$$\xi_k(\mathbf{y}_k) = \frac{1}{(2\pi d_{k1}^2)^{3/4}} \exp[-\mathbf{y}_k^2/4d_{k1}^2]$$

and (4.6)

$$\zeta_k(\mathbf{z}_k) = \frac{1}{(2\pi d_{k2}^2)^{3/4}} \exp[-\mathbf{z}_k^2/4d_{k2}^2].$$

Neglecting annihilation, the mesons represented by ξ_1, ζ_1, ξ_3 , and ζ_3 have one light and one strange particle. On the other hand, that denoted by ξ_2 has both particles as light ones (up or down) and ζ_2 has two heavier particles. It follows thus from the properties of the solutions of a three-dimensional (3D) harmonic oscillator that d_{11}, d_{12}, d_{31} , and d_{32} have a particular value, say, d' , d_{21} has a different one d , and d_{22} differs from all these, having a value denoted by d'' . Quantitatively

$$\frac{d'^2}{d^2} = \sqrt{\frac{m(m_s + m)}{2mm_s}} = \sqrt{\frac{s+1}{2s}}$$

and (4.7)

$$\frac{d''^2}{d^2} = \sqrt{\frac{2m}{2m_s}} = \sqrt{\frac{1}{s}}.$$

It is to be noted that here we are neglecting the spin dependence of the size of a cluster. For the absolute magnitudes of the sizes, the equation $d^2 = \sqrt{3}R_n^2/2$ is used relating the radius of a meson composed of the light mesons to the rms charge radius $R_n=0.6$ fm of a nucleon whose qqq wave function is generated by the same quadratic confining potential.

Where the annihilation processes are incorporated, things are a bit different: the flavor wave function gets mixed with the quark position-dependent part. This follows because the size of a mesonic cluster depends upon the masses of the particles it contains. Thus in the (pseudoscalar-pseudoscalar) $2S$ channel, where the pairs $(2, \bar{3})$ and $(1, \bar{4})$ become actually mixtures of $s\bar{s}$, $u\bar{u}$, and $d\bar{d}$ resulting in η, η' , or π , we have to use instead of ξ_2 and ζ_2 their corresponding mixtures (termed quark-flavor wave functions in the following). Depending upon the physical mesons taking part in the scattering process, these are

$$|2S\rangle_{fq} = \begin{cases} \begin{cases} |\eta'_{1\bar{4}}\rangle_{fq} |\eta'_{2\bar{3}}\rangle_{fq} & \text{for } \eta'\eta' \text{ mesons,} \\ |\eta_{1\bar{4}}\rangle_{fq} |\eta_{2\bar{3}}\rangle_{fq} & \text{for } \eta\eta' \text{ mesons,} \\ |\eta_{1\bar{4}}\rangle_{fq} |\eta_{2\bar{3}}\rangle_{fq} & \text{for } \eta\eta' \text{ mesons,} \\ |\pi_{1\bar{4}}\rangle_{fq} |\eta_{2\bar{3}}\rangle_{fq} & \text{for } \pi\eta' \text{ mesons,} \\ |\pi_{1\bar{4}}\rangle_{fq} |\eta_{2\bar{3}}\rangle_{fq} & \text{for } \pi\eta \text{ mesons,} \end{cases} \text{ or } \begin{cases} |\eta'_{1\bar{4}}\rangle_{fq} |\eta_{2\bar{3}}\rangle_{fq} & \text{for } \eta\eta' \text{ mesons,} \\ |\eta_{1\bar{4}}\rangle_{fq} |\eta_{2\bar{3}}\rangle_{fq} & \text{for } \eta\eta' \text{ mesons,} \\ |\pi_{1\bar{4}}\rangle_{fq} |\eta_{2\bar{3}}\rangle_{fq} & \text{for } \pi\eta' \text{ mesons,} \\ |\pi_{1\bar{4}}\rangle_{fq} |\eta_{2\bar{3}}\rangle_{fq} & \text{for } \pi\eta \text{ mesons,} \end{cases} \end{cases} \quad (4.8)$$

with

$$|\eta_{ij}\rangle_{fq} = \cos\theta \frac{|d\bar{d} + u\bar{u}\rangle_f}{\sqrt{2}} \xi_2(\mathbf{r}_{ij}) - \sin\theta |s\bar{s}\rangle_f \zeta_2(\mathbf{r}_{ij}),$$

$$|\eta'_{ij}\rangle_{fq} = \sin\theta \frac{|d\bar{d} + u\bar{u}\rangle_f}{\sqrt{2}} \xi_2(\mathbf{r}_{ij}) + \cos\theta |s\bar{s}\rangle_f \zeta_2(\mathbf{r}_{ij}),$$
(4.9)

$$|\pi_{1\bar{4}}\rangle_{fq} = |\pi\rangle_f \xi_2(\mathbf{r}_{1\bar{4}}) = |\pi\rangle_f \xi_2(\mathbf{y}_2). \quad (4.10)$$

Here

$$\xi_2(\mathbf{r}_{ij}) = \frac{1}{(2\pi d_{21}^2)^{3/4}} \exp[-\mathbf{r}_{ij}^2/4d_{21}^2]$$
(4.11)

and

$$\zeta_2(\mathbf{r}_{ij}) = \frac{1}{(2\pi d_{22}^2)^{3/4}} \exp[-\mathbf{r}_{ij}^2/4d_{22}^2],$$

where $d_{21} = d$, $d_{22} = d''$, and θ ($= 34.7^\circ$) is related to the mixing angle $\theta_P = -20^\circ$ of the flavor singlet and octet resulting in η and η' (see pp. III.68 and III.69 of [26]).

Now we write the Schrödinger equation for the system in hand:

$$(H - E_c)|\Psi(q_1, q_2, \bar{q}_3, \bar{q}_4; g)\rangle = 0, \quad (4.12)$$

where H is the total Hamiltonian and E_c is the total center-of-mass energy of the $q^2\bar{q}^2$ system. The above equation also means that the overlap of $(H - E_c)|\Psi\rangle$ with an arbitrary variation $|\delta\Psi\rangle$ of the state vector $|\Psi\rangle$ vanishes. In $|\delta\Psi\rangle$ we consider, as in resonating group method calculations, only the variations in χ_{kI} [see Eq. (4.5)]. Thus we write

$$\langle \delta\Psi | H - E_c | \Psi \rangle = \sum_{kIJ} \int d^3\mathbf{R}_c d^3\mathbf{y}_k d^3\mathbf{z}_k \psi_c(\mathbf{R}_c) \delta\chi_{kI}(\mathbf{R}_k) \xi_k(\mathbf{y}_k) \zeta_k(\mathbf{z}_k) \times \langle f | k | s \langle kI | g \langle k | H - E_c | l \rangle g | lJ \rangle s | l \rangle_f \psi_c(\mathbf{R}_c) \chi_{lJ}(\mathbf{R}_l) \xi_l(\mathbf{y}_l) \zeta_l(\mathbf{z}_l) = 0. \quad (4.13)$$

To do these four space integrations, any of the three sets of vectors defined by Eqs. (4.2), (4.3), and (4.4) can be used. The choice $\mathbf{R}_k, \mathbf{y}_k$, and \mathbf{z}_k has, however, a clear advantage. The arbitrary variations $\delta\chi_{kI}(\mathbf{R}_k)$'s for different (but continuous) values of \mathbf{R}_k are linearly independent and hence their coefficients in Eq. (4.13) should be zero. With the trivial \mathbf{R}_c integration performed to give a finite result using, say, box normalization, this leads to

$$\sum_{IJ} \int d^3\mathbf{y}_k d^3\mathbf{z}_k \xi_k(\mathbf{y}_k) \zeta_k(\mathbf{z}_k) \times \langle f | k | s \langle kI | g \langle k | H - E_c | l \rangle g | lJ \rangle s | l \rangle_f \times \chi_{lJ}(\mathbf{R}_l) \xi_l(\mathbf{y}_l) \zeta_l(\mathbf{z}_l) = 0, \quad (4.14)$$

for $k, l = 1, 2$, or 3 and $I, J = S$ or T (except where annihilation is considered).

By Eq. (3.6), H in the above is $K(f) + V^P(f) + V^a + \sum_{i=1}^4 m_i$, with $V^P(f) = V^{cf}(f) + V^{hyp}(f)$. Using Eqs. (3.7) and (3.8) for $V^{cf}(f)$ and $V^{hyp}(f)$, respectively, the matrix elements of $V^P(f)$ in our spin basis are given by

$${}_s\langle X | V^P(f) | X' \rangle_s = \sum_{i < j} \mathbf{F}_i \cdot \mathbf{F}_j(f) (V_{ij})_{X_s, X'_s}, \quad (4.15)$$

with

$$(V_{ij})_{X_s, X'_s} = v_{ij} {}_s\langle X | X' \rangle_s - \frac{8\pi\alpha_s^{ij}}{3m_i m_j} \delta^3(\mathbf{r}_{ij}) \times {}_s\langle X | \mathbf{S}_i \cdot \mathbf{S}_j | X' \rangle_s. \quad (4.16)$$

In this form, ${}_s\langle X | V^P | X' \rangle_s$ is very similar to V^{cf} appearing in Eq. (2.2). So its matrix elements between the gluonic states are the same as those of V^{cf} except for the new spin-dependent coefficients V_{ij} replacing v_{ij} . Thus $V^P(f)$ is [compare with Eq. (2.12)]

$$V^P(f) = \begin{pmatrix} -\frac{4}{3}(V_{13} + V_{24})_{1,1} & \frac{4f}{9} \begin{pmatrix} V_{12} + V_{34} \\ -V_{13} - V_{24} \\ -V_{14} - V_{23} \end{pmatrix}_{1,2} & \frac{2f}{3\sqrt{3}} \begin{pmatrix} -2(V_{13} + V_{24}) \\ +V_{14} + V_{23} \\ -V_{12} - V_{34} \end{pmatrix}_{1,3} \\ & -\frac{4}{3}(V_{14} + V_{23})_{2,2} & \frac{2f}{3\sqrt{3}} \begin{pmatrix} 2(V_{14} + V_{23}) \\ +V_{12} + V_{34} \\ -V_{24} - V_{13} \end{pmatrix}_{2,3} \\ \text{symmetric} & & -\frac{1}{3} \begin{pmatrix} 2(V_{12} + V_{34}) \\ +V_{13} + V_{24} \\ +V_{14} + V_{23} \end{pmatrix}_{3,3} \\ & & +\frac{5}{2} I D f (1 - f) \end{pmatrix}, \quad (4.17)$$

in our six-dimensional gluonic-spin basis $|1\rangle_g|1S\rangle_s$, $|1\rangle_g|1T\rangle_s, \dots, |3\rangle_g|3T\rangle_s$.

As written above, $V^p(f)$ has only *nine* elements, rather than 36. Actually, every term in the above is meant to stand for a 2×2 matrix defined by

$$(V_{ij})_{k,l} = \begin{pmatrix} (V_{ij})_{kS,lS} & (V_{ij})_{kS,lT} \\ (V_{ij})_{kT,lS} & (V_{ij})_{kT,lT} \end{pmatrix}, \quad (4.18)$$

for $k, l=1, 2$, or 3 . $(V_{ij})_{kI,lJ}$ is given through Eq. (4.16)

$$\sum_{IJ} \int d^3\mathbf{R}_l \left[\mathcal{K}_{kI,lJ}(\mathbf{R}_k, \mathbf{R}_l) + \mathcal{V}_{kI,lJ}^{\text{cf}}(\mathbf{R}_k, \mathbf{R}_l) + \mathcal{V}_{kI,lJ}^{\text{hyp}}(\mathbf{R}_k, \mathbf{R}_l) - \left(E_c - \sum_{i=1}^4 m_i \right) \mathcal{N}_{kI,lJ}(\mathbf{R}_k, \mathbf{R}_l) \right] \chi_{lJ}(\mathbf{R}_l) = 0, \quad (4.19)$$

for $l = 1, 2$, and 3 along with $J = S$ and T . This gives six equations, for the same three values of k and two of I . Here $\mathcal{K}_{kI,lJ}$, $\mathcal{V}_{kI,lJ}^{\text{cf}}$, $\mathcal{V}_{kI,lJ}^{\text{hyp}}$ and $\mathcal{N}_{kI,lJ}$, are defined by

$$\begin{aligned} & \int d^3\mathbf{R}'_l \mathcal{K}_{kI,lJ}(\mathbf{R}_k, \mathbf{R}'_l) \chi_{lJ}(\mathbf{R}'_l) \\ &= \int d^3\mathbf{y}_k d^3\mathbf{z}_k \xi_k(\mathbf{y}_k) \zeta_k(\mathbf{z}_k) K_{kI,lJ} \chi_{lJ}(\mathbf{R}_l) \xi_l(\mathbf{y}_l) \zeta_l(\mathbf{z}_l), \end{aligned} \quad (4.20)$$

$$\begin{aligned} & \int d^3\mathbf{R}'_l \mathcal{V}_{kI,lJ}^{\text{cf}}(\mathbf{R}_k, \mathbf{R}'_l) \chi_{lJ}(\mathbf{R}'_l) \\ &= \int d^3\mathbf{y}_k d^3\mathbf{z}_k \xi_k(\mathbf{y}_k) \zeta_k(\mathbf{z}_k) V_{kI,lJ}^{\text{cf}} \chi_{lJ}(\mathbf{R}_l) \xi_l(\mathbf{y}_l) \zeta_l(\mathbf{z}_l), \end{aligned} \quad (4.21)$$

$$\begin{aligned} & \int d^3\mathbf{R}'_l \mathcal{V}_{kI,lJ}^{\text{hyp}}(\mathbf{R}_k, \mathbf{R}'_l) \chi_{lJ}(\mathbf{R}'_l) \\ &= \int d^3\mathbf{y}_k d^3\mathbf{z}_k \xi_k(\mathbf{y}_k) \zeta_k(\mathbf{z}_k) V_{kI,lJ}^{\text{hyp}} \chi_{lJ}(\mathbf{R}_l) \xi_l(\mathbf{y}_l) \zeta_l(\mathbf{z}_l), \end{aligned} \quad (4.22)$$

$$\begin{aligned} & \int d^3\mathbf{R}'_l \mathcal{N}_{kI,lJ}(\mathbf{R}_k, \mathbf{R}'_l) \chi_{lJ}(\mathbf{R}'_l) \\ &= \int d^3\mathbf{y}_k d^3\mathbf{z}_k \xi_k(\mathbf{y}_k) \zeta_k(\mathbf{z}_k) N_{kI,lJ} \chi_{lJ}(\mathbf{R}_l) \xi_l(\mathbf{y}_l) \zeta_l(\mathbf{z}_l), \end{aligned} \quad (4.23)$$

with $K_{kI,lJ}$, $V_{kI,lJ}^{\text{cf}}$, and $V_{kI,lJ}^{\text{hyp}}$ as the matrix elements of the $K(f)$, $V^{\text{cf}}(f)$, and $V^{\text{hyp}}(f)$. $N_{kI,lJ}$ is the overlap of the spin-gluonic states appearing in Eq. (4.14), calculated using the results mentioned in Sec. II along with those in Appendix A for the spin overlap factor ${}_s\langle kI|lJ\rangle_s$.

The spatial integrations appearing on the right-hand side (RHS) of Eqs. (4.20) – (4.23) were done differently

and I multiplying the D term in the (3,3) element of Eq. (4.17) is a 2×2 identity matrix. To determine the overlap of any two spin states and the corresponding matrix element of $\mathbf{S}_i \cdot \mathbf{S}_j$, the definitions given through Eqs. (3.1), (3.2), and (3.3) have to be used. The results thus obtained are reported in Appendix A.

As far as the spin dependence is concerned, the other terms in the Hamiltonian are unit operators. Using the results from Sec. II for the matrix elements between the gluonic states, we write Eq. (4.14) as

for the diagonal ($k = l$) and off-diagonal ($k \neq l$) terms. In the former case, $\chi_{lJ}(\mathbf{R}_l)$ is linearly independent of the integration variables \mathbf{y}_k and \mathbf{z}_k and thus was simply taken out of the integrations. In the case of off-diagonal terms, the integration variables (\mathbf{y}_k and \mathbf{z}_k) were replaced by their equivalent combinations with one identical to \mathbf{R}_l , and the other one independent of it. Integrating out the vector independent of \mathbf{R}_l and expressing the remaining one on the RHS in terms of \mathbf{R}_k and \mathbf{R}_l , we got results for $\mathcal{K}_{kI,lJ}$, $\mathcal{V}_{kI,lJ}^{\text{cf}}$, $\mathcal{V}_{kI,lJ}^{\text{hyp}}$, and $\mathcal{N}_{kI,lJ}$ after comparing with the LHS of the corresponding equation.

Where annihilation is considered, we have to use the combined quark and flavor wave functions $|2S\rangle_{fq}$ instead of $\xi_2\zeta_2$. Thus in the $2S$ channel diagonal term we have, in place of the $k = l = 2$ and $I = J = S$ term in Eq. (4.14),

$$\begin{aligned} & \int d^3\mathbf{r}_{1\bar{4}} d^3\mathbf{r}_{2\bar{3}} {}_{fq}\langle 2S| {}_s\langle 2S| {}_g\langle 2| K + V^{\text{cf}} + V^{\text{hyp}} \\ & - \left(E_c - \sum_{i=1}^4 m_i \right) |2\rangle_g |2S\rangle_s |2S\rangle_{fq} \chi_{2S}(\mathbf{R}_2) \\ & + \int d^3\mathbf{r}_{1\bar{4}} d^3\mathbf{r}_{2\bar{3}} {}_{fq}\langle 2S| V^a |2S\rangle_{fq} \chi_{2S}(\mathbf{R}_2). \end{aligned} \quad (4.24)$$

As Eq. (4.8) shows, the form of $|2S\rangle_{fq}$ depends upon the physical content of the $2S$ channel. This would result in different expressions for each of $\mathcal{K}_{2S,2S}$, $\mathcal{V}_{2S,2S}^{\text{cf}}$, $\mathcal{V}_{2S,2S}^{\text{hyp}}$, and $\mathcal{N}_{2S,2S}$ for different pairs of mesons in the channel. In the following calculations we restrict ourselves to just some lower channels: $\eta\eta$ in the isoscalar, plus $\eta\pi$ and $\eta'\pi$ in the isovector sector. This is done because of our special interest in the behavior of the $K\bar{K}$ system near the threshold (see the next section).

The results thus obtained for the kernels appearing in Eq. (4.19) are reported in Appendix B. Substitution of these in Eq. (4.19) would give *six* coupled equations. However, we neglect all connections to the third gluonic channel. This is justified to some extent by the absence of any significant effect of removing the third channel in the spinless case (see Fig. 4 of [11]), meaning that the gluonic effects represented by the third channel are small

compared with those incorporated through multiplying the remaining off-diagonal elements (i.e., 1,2, and 2,1) by the space-dependent f factor. This neglect leaves us with just *four* equations [two of these are written below as Eqs. (4.27) and (4.28)]. The off-diagonal terms in these equations tend to zero for large intercluster distances. Thus for consistency with the observed meson spectroscopy we require the constant term in each of the diagonal parts to be equal to the sum of masses of the corresponding mesons. Fitting in this way to the masses of $K, \eta, \eta', \pi, K^*, \omega$ (or ρ), and ϕ mesons, we get the following values of the above mentioned free parameters:

$$\begin{aligned} m &= 277 \text{ MeV}, & s &= 1.955, & \bar{C} &= 456 \text{ MeV}, \\ \alpha_s^{ll} &= 1.583, & \alpha_s^{ls} &= 1.561, & \alpha_s^{ss} &= 1.501, \\ a_1 &= 272 \text{ MeV}, & \text{and} & & a_s &= 67.4 \text{ MeV}. \end{aligned} \quad (4.25)$$

For C [see Eq. (2.3)], the equality of kinetic and potential energies of a harmonic oscillator is used, giving

$$C = -\frac{1}{4d^2} \frac{3}{4} \omega_2^2 = -\frac{3}{16md^4} = -270 \text{ MeV/fm}^2. \quad (4.26)$$

After this parameter fit (except for \bar{k} to be discussed in the next section), we write down *two* of the *four* coupled equations mentioned above. The remaining two equations would involve vector mesons. These are not incorporated beyond this stage because of our above mentioned neglect of channels opening at energies significantly higher than the $K\bar{K}$ threshold:

$$\begin{aligned} & \left[M_K + M_{\bar{K}} - \frac{1}{2\mu_{K\bar{K}}} \nabla_{\mathbf{R}_1}^2 - E_c \right] \chi_{1S}(\mathbf{R}_1) \\ & + e_0 \int d^3 \mathbf{R}_2 \left\{ \left[-\frac{1}{2m} \frac{1}{6} (q_{11} \mathbf{R}_1^2 + q_{12} \mathbf{R}_2^2 + q_{10}) + C(\mathbf{R}_1) \right] \exp[-e_2 \mathbf{R}_2^2 - e_1 \mathbf{R}_1^2] - G(\mathbf{R}_1, \mathbf{R}_2) H \right\} \chi_{2S}(\mathbf{R}_2) = 0, \end{aligned} \quad (4.27)$$

and

$$\begin{aligned} & \left[M_a + M_b - \frac{1}{2\mu_{ab}} \nabla_{\mathbf{R}_2}^2 - E_c \right] \chi_{2S}(\mathbf{R}_2) \\ & + e_0 \int d^3 \mathbf{R}_1 \left\{ \left[-\frac{1}{2m} \frac{1}{6} (q_{21} \mathbf{R}_1^2 + q_{22} \mathbf{R}_2^2 + q_{20}) + C(\mathbf{R}_1) \right] \exp[-e_2 \mathbf{R}_2^2 - e_1 \mathbf{R}_1^2] - G(\mathbf{R}_1, \mathbf{R}_2) H \right\} \chi_{1S}(\mathbf{R}_1) = 0, \end{aligned} \quad (4.28)$$

for $K\bar{K} \leftrightarrow ab$, where a and b are the two mesons in the second channel ($\eta\eta, \eta\pi$, or $\eta'\pi$). Here

$$C(\mathbf{R}_1) = \frac{1}{2} (b_1 \mathbf{R}_1^2 + b_0) - \frac{1}{6} [E_c + \frac{8}{3} \bar{C} - 2m(s+1)] \quad (4.29)$$

$$\begin{aligned} G(\mathbf{R}_1, \mathbf{R}_2) &= l_{10} \exp[-(e_1 + e'_1 - l_{11}) \mathbf{R}_1^2 - (e_2 + l_{12}) \mathbf{R}_2^2] [\alpha_s^{ls} \exp(l_{13} \mathbf{R}_1 \cdot \mathbf{R}_2) + \alpha_s^{ls} \exp(-l_{13} \mathbf{R}_1 \cdot \mathbf{R}_2)] \\ &+ l_{20} \exp[-(e_1 + e'_1 + l_{21}) \mathbf{R}_1^2 - e_2 \mathbf{R}_2^2] [\alpha_s^{ll} \exp(l_{22} \mathbf{R}_1^2) + s \alpha_s^{ss} \exp(-l_{22} \mathbf{R}_1^2)] \\ &+ l_{30} \exp[-(e_1 + e'_1 + l_{31}) \mathbf{R}_1^2 - (e_2 + l_{32}) \mathbf{R}_2^2] [\alpha_s^{ls} \exp(l_{33} \mathbf{R}_1 \cdot \mathbf{R}_2) + \alpha_s^{ls} \exp(-l_{33} \mathbf{R}_1 \cdot \mathbf{R}_2)], \end{aligned} \quad (4.30)$$

$$H = \frac{1}{6} \frac{8\pi}{3m^2 s} \frac{(2\kappa)^{3/2}}{(2\pi d^2)^{3/2}}. \quad (4.31)$$

It should be noted that in the coefficients of $\nabla_{\mathbf{R}_1}^2$ and $\nabla_{\mathbf{R}_2}^2$ the reduced masses of the corresponding mesons now appear. This is done so as to ensure that the terms involving $\nabla_{\mathbf{R}_1}^2$ or $\nabla_{\mathbf{R}_2}^2$ give the correct kinetic energy of the relative motion of the interacting physical mesons. Other symbols appearing in the above equations are defined in Appendix B at appropriate places.

The kernels in the off-diagonal parts in the above coupled equations contain nonseparable parts $\exp(l_{13} \mathbf{R}_1 \cdot \mathbf{R}_2) \cdots \exp(l_{33} \mathbf{R}_1 \cdot \mathbf{R}_2)$. The presence of these "nonseparable potentials" makes the solution of these equations rather involved. To avoid that complication, we can solve

our problem after replacing these terms by their truncated expansions. This would leave us with an inexact but manageable form of the equations. With that strategy in mind, the above equations were solved first for the case of no hyperfine interaction by setting $H = 0$ in the above two coupled equations. The method used for that is explained below for the full interaction case. The resulting phase shifts for this no hyperfine case (some of these are reported in the next section) are so small that it would be a good approximation to take the variational wave functions $\chi_{1S}(\mathbf{R}_1)$ and $\chi_{2S}(\mathbf{R}_2)$ in the *absence* of hyperfine interaction as the wave functions correspond-

ing to a freely propagating plane wave. Using, initially, this approximation for $\chi_{1S}(\mathbf{R}_1)$ and $\chi_{2S}(\mathbf{R}_2)$ even in the presence of hyperfine interaction, we looked for a reasonable separable approximation to our nonseparable terms. As far as $\exp(l_{13}\mathbf{R}_1 \cdot \mathbf{R}_2)$ and $\exp(-l_{13}\mathbf{R}_1 \cdot \mathbf{R}_2)$ are con-

cerned, it was seen to be a very good approximation to just replace them with the exponential expansion up to the second power in $l_{13}\mathbf{R}_1 \cdot \mathbf{R}_2$. But the terms multiplying l_{30} are not so easy to manage. For them we used

$$l_{30} \exp [-(e_1 + e'_1 + l_{31})\mathbf{R}_1^2 - (e_2 + l_{32})\mathbf{R}_2^2] \{ \alpha_s^{l_s} \exp(-l_{33}\mathbf{R}_1 \cdot \mathbf{R}_2) + \alpha_s^{l_s} \exp(l_{33}\mathbf{R}_1 \cdot \mathbf{R}_2) \} \\ \approx n_1 l_{30} \alpha_s^{l_s} \{ \exp[-\tau_1(e_1 + e'_1 + l_{31} + e_2 + l_{32} - l_{33})(R_1^2 + R_2^2)] - [-\tau_1(e_1 + e'_1 + l_{31} + e_2 + l_{32} + l_{33})(R_1^2 + R_2^2)] \}, \quad (4.32)$$

in Eq. (4.27), n_1 and τ_1 being two new (energy-dependent) parameters. In Eq. (4.28) two similar parameters, denoted by n_2 and τ_2 , were used.

To check how good this approximation is, both sides of Eq. (4.32), multiplied by $R_2^2 \chi_{2S}(R_2)$ and integrated over R_2 , were plotted as functions of R_1 . This showed that by adjusting n_1 and τ_1 even the worst discrepancy could be reduced to less than 10% of the total hyperfine coupling for that particular value of R_1 and the on-shell momentum $p_c(2)$. But that adjustment was done with a rather poor (i.e., plane wave) approximation for $\chi_{2S}(R_2)$. Equation (4.28) was treated similarly. So when, after calculating the T and S scattering matrices, the results were checked for unitarity of the S matrix and symmetry of the T matrix (required by "reciprocity" of inelastic scattering; see, for example, p. 528 of [27]), the discrepancy was for some cases as bad as 30%. This means that the above approximation needs to be improved, for example, by iterating it many times, before meaningful results for phase shifts are obtained. This improvement remains to be made, though this problem does *not* affect our main results. This is because this readjusting of the values of n_1, n_2, τ_1 , and τ_2 [with improved functional dependences

of $\chi_{1S}(\mathbf{R}_1)$ and $\chi_{2S}(\mathbf{R}_2)$] is *not* needed for the range of energy where our immediate interest lies (i.e., below the KK threshold in the first channel). This follows because the momentum space solutions [see Eqs. (4.33) and (4.34) below] of the above coupled equations for that range of energy are of the form

$$\chi(p) = -\frac{1}{\Delta(p)} \times \text{const.}$$

Changing values of n_1, τ_1, n_2 , and τ_2 in that situation would just affect the constant coefficients of $\frac{1}{\Delta_1(p_1)}$ and $\frac{1}{\Delta_2(p_2)}$, leaving the momentum dependence of the solutions χ_{1S} and χ_{2S} unchanged.

With the above replacement the integrands appearing in Eqs. (4.27) and (4.28) are products of two factors, each of them a function of R_1 or R_2 . This means that in this form the two coupled equations can be solved exactly, using the method demonstrated in Appendix B of [11]. So we first wrote Eqs. (4.27) and (4.28), in the approximate form [see Eq. (4.32)], in momentum space. For incoming waves in the first channel, the formal momentum space solution of these equations would be

$$\chi_{1S}(p_1) = \frac{\delta(p_1 - p_c(1))}{p_c^2(1)} - \frac{1}{\Delta_1(p_1)} \left[Q_1^{(1)} A_2(e_2) + Q_2^{(1)} B_2(e_2) + Q_3^{(1)} A_2(e_2 + l_{12}) + Q_4^{(1)} B_2(e_2 + l_{12}) \right. \\ \left. + Q_5^{(1)} A_2(\tau_1 e_1 + e'_1 + l_{31} + e_2 + l_{32} - l_{33}) + Q_6^{(1)} A_2(\tau_1 e_1 + e'_1 + l_{31} + e_2 + l_{32} + l_{33}) \right], \quad (4.33)$$

$$\chi_{2S}(p_2) = -\frac{1}{\Delta_2(p_2)} \left[Q_1^{(2)} A_1(e_1) + Q_2^{(2)} B_1(e_1) + Q_3^{(2)} A_1(e_1 + e'_1 + l_{21} - l_{22}) + Q_4^{(2)} A_1(e_1 + e'_1 + l_{21} + l_{22}) \right. \\ \left. + Q_5^{(2)} A_1(e_1 + e'_1 - l_{11}) + Q_6^{(2)} B_1(e_1 + e'_1 - l_{11}) + Q_7^{(2)} A_1(\tau_2 e_1 + e'_1 + l_{31} + e_2 + l_{32} - l_{33}) \right. \\ \left. + Q_8^{(2)} A_1(\tau_2 e_1 + e'_1 + l_{31} + e_2 + l_{32} + l_{33}) \right]. \quad (4.34)$$

The new symbols appearing in these equations are defined in Appendix C.

It is to be noted that in the above equations \mathbf{p}_1 and \mathbf{p}_2 have been replaced everywhere by p_1 and p_2 , respectively, utilizing the spherical symmetry of our problem. Multiplying Eq. (4.33) by $p_1^2 F_a(p_1, e_1)$, $p_1^2 F_b(p_1, e_1)$, $p_1^2 F_a(p_1, e_1 + e'_1 + l_{21} - l_{22})$, $p_1^2 F_a(p_1, e_1 + e'_1 + l_{21} + l_{22})$, $p_1^2 F_a(p_1, e_1 + e'_1 - l_{11})$, $p_1^2 F_b(p_1, e_1 + e'_1 - l_{11})$, $p_1^2 F_a(p_1, \tau_2 e_1 + e'_1 + l_{31} + e_2 + l_{32} - l_{33})$, and $p_1^2 F_a(p_1, \tau_2 e_1 + e'_1 + l_{31} + e_2 + l_{32} + l_{33})$ in turn and integrating with respect to p_1 gives us eight equations ($F_a(p_1, x)$ and $F_b(p_1, x)$ are the Fourier transforms of $\exp[-xR_1^2]$ and $R_1^2 \exp[-xR_1^2]$, respectively). Similarly, multiplying Eq. (4.34) by the Fourier transforms $p_2^2 F_a(p_2, e_2)$, $p_2^2 F_b(p_2, e_2)$, $p_2^2 F_a(p_2, e_2 + l_{12})$, $p_2^2 F_b(p_2, e_2 + l_{12})$, $p_2^2 F_a(p_2, \tau_1 e_1 + e'_1 + l_{31} + e_2 + l_{32} - l_{33})$, and $p_2^2 F_a(p_2, \tau_1 e_1 + e'_1 + l_{31} + e_2 + l_{32} + l_{33})$ and integrating with respect to p_2 gives us six more equations. These 14 equations can be written as a matrix equation

$$QU_1 = U_2 \tag{4.35}$$

with

$$U_2 = 4\pi \begin{pmatrix} F_a(p_c(1), e_1) \\ F_b(p_c(1), e_1) \\ F_a(p_c(1), e_1 + e'_1 + l_{21} - l_{22}) \\ F_a(p_c(1), e_1 + e'_1 + l_{21} + l_{22}) \\ F_a(p_c(1), e_1 + e'_1 - l_{11}) \\ F_b(p_c(1), e_1 + e'_1 - l_{11}) \\ F_a(p_c(1), \tau_2 e_1 + e'_1 + l_{31} + e_2 + l_{32} - l_{33}) \\ F_a(p_c(1), \tau_2 e_1 + e'_1 + l_{31} + e_2 + l_{32} + l_{33}) \\ 0 \\ 0 \\ 0 \\ 0 \\ 0 \\ 0 \end{pmatrix}, \tag{4.36}$$

Q a 14 × 14 matrix containing many integrals, and U₁ a vector containing

$$A_2(e_2), B_2(e_2), \dots, A_2(\tau_1 e_1 + e'_1 + l_{31} + e_2 + l_{32} + l_{33})$$

and

$$A_1(e_1), B_1(e_1), \dots, A_1(\tau_2 e_1 + e'_1 + l_{31} + e_2 + l_{32} + l_{33})$$

as its elements. Inverting the matrix Q gives these 14 elements of the U₁ vector. With these values in hand, all the quantities in the expressions for χ_{1S}(p₁) and χ_{2S}(p₂) are known. So these can now simply be obtained by making in Eqs. (4.33) and (4.34) the usual replacement of p₁ and p₂ by their on-shell values p_c(1) and p_c(2), defined by Eqs. (C9) and (C10).

From Eqs. (4.33) and (4.34) the two T matrix elements T_{1,1} and T_{2,1} can be read off as (apart from a constant) coefficients of the nonrelativistic Green operators $-\frac{1}{\Delta_1(p_1)}$ and $-\frac{1}{\Delta_2(p_2)}$. These are reported in Appendix D. Similarly, for incoming waves in channel 2, the use of U₂ as

$$U_2 = 4\pi \begin{pmatrix} 0 \\ 0 \\ 0 \\ 0 \\ 0 \\ 0 \\ 0 \\ 0 \\ F_a(p_c(2), e_2) \\ F_b(p_c(2), e_2) \\ F_a(p_c(2), e_2 + l_{12}) \\ F_b(p_c(2), e_2 + l_{12}) \\ F_a(p_c(2), \tau_1 e_1 + e'_1 + l_{31} + e_2 + l_{32} - l_{33}) \\ F_a(p_c(2), \tau_1 e_1 + e'_1 + l_{31} + e_2 + l_{32} + l_{33}) \end{pmatrix} \tag{4.37}$$

gives the two T matrix elements T_{2,2} and T_{1,2} also reported in Appendix D.

For the total energy in the center-of-mass frame above the higher threshold, both of the channels would be open. Thus for incoming waves in either of them, there would be a loss of flux in the incoming channel. Representing this *inelasticity* by a factor ε_k, for k = 1 or 2, we can write

$$S_{1,1} = 1 - 2iT_{1,1} = \epsilon_1 e^{2i\delta_1}, \tag{4.38}$$

$$S_{2,2} = 1 - 2iT_{2,2} = \epsilon_2 e^{2i\delta_2}. \tag{4.39}$$

For elastic scattering, ε₁ or ε₂ would be unity for incoming waves in channel 1 or 2, respectively.

Below the lower threshold the situation is qualitatively different as, with both p_c(1) and p_c(2) being imaginary,

TABLE I. Increases in the couplings necessary to get binding. BE denotes binding energy.

\bar{k} (fm^{-2})	Hyperfine coupling			Increase in the total coupling to get binding	Increase without hyperfine to get binding
	Increase to get binding	BE in the isovector channel (MeV)	BE in the isoscalar channel (MeV)		
0	1.926	<1	35	2.715	3.06
1/6	3.00	<1	53	4.26	6.57
1/2	6.43	<1	87	8.89	19.13

$\delta(p_1 - p_c(1))$ and $\delta(p_2 - p_c(2))$ do not contribute to the integration over all the real values of p_1 and p_2 performed to arrive at Eq. (4.35). Thus all the terms collected in the vector U_2 would be absent, leaving us instead with

$$QU_1 = 0. \quad (4.40)$$

A nontrivial solution of this equation for the elements of the vector U_1 requires

$$\det Q = 0, \quad (4.41)$$

giving us a condition for the existence of a bound state of the whole system.

V. RESULTS

The formalism presented in this paper can describe a number of meson-meson systems. Amongst these systems we have chosen $K\bar{K}$, keeping in mind that it has been investigated by other groups using different models for the quark-quark interaction. An important issue is whether the whole $K\bar{K}$ system has a bound state just below the $K\bar{K}$ threshold or not. According to our method, this depends upon whether or not Eq. (4.41) is satisfied. The Q matrix there is actually a complicated function of the parameters of the formalism and the total energy of the whole system. These parameters are fitted above, except \bar{k} [see Eq. (2.7)] which is the parameter of our model of the gluonic effects. Our numerical calculations were done for three values of \bar{k} in turn. The value $\bar{k} = 0$ corresponds to a two-body potential model Hamiltonian. On the other hand, $\bar{k} = 1/2 \text{ fm}^{-2}$ is emerging from the lattice gauge theory calculations [22] for rectangular configurations of quark positions. For other configurations,

indications [23] are that the spatial decrease of gluonic topologies overlap may be slower, and thus we have also used an intermediate value ($\bar{k} = 1/6 \text{ fm}^{-2}$). Which of these, if any, would simulate the “experimental” (lattice-gauge-theory-based) behavior of the gluonic overlap is yet to be seen.

Our numerical calculations showed that, for any value of \bar{k} , the above condition for the existence of a bound state [see Eq. (4.41)] is *not* satisfied for any value of energy below the $K\bar{K}$ threshold. This is the situation in the isoscalar as well as in the isovector sector, whereas in the latter case all connections to the $\pi\eta$ channel are neglected as those would not affect the answer to the main question being discussed here. On the other hand, using a closely related model Weinstein and Isgur [7] get $K\bar{K}$ bound states in both the isoscalar and the isovector sectors, and conclude that the two scalar meson resonances $f_0(975)$ and $a_0(980)$ can be explained as loosely bound $K\bar{K}$ states. Their model corresponds, in some approximation (see the first paragraph of the next section), to ours in the limit $\bar{k} = 0$. Therefore it is interesting to see if, in the corresponding limit, we can get their results by varying our parameters. Our calculations showed that for $\bar{k} = 0$ we need to multiply our total couplings of the two channels by a factor of 2.715 before we can get bound states in both the isoscalar and isovector sectors. Alternatively, we can get these bound states by multiplying *only* the hyperfine couplings by a factor of 1.926. We get bound states without hyperfine interaction as well, but for that an increase by a factor of 3.06 in the remaining couplings is needed. This is one of the indications in our work that the hyperfine coupling is the main interaction arising through quark exchange, and that the hyperfine and other couplings have opposite signs.

Our modification to the two-body potential model pro-

TABLE II. Isovector phase shifts.

E_c (total c.m. energy) (MeV)	\bar{k} (fm^{-2})	Full coupling		Without hyperfine			
		δ_1 (deg)	ϵ_1	δ_2 (deg)	δ_1 (deg)	ϵ_1	δ_2 (deg)
1042.0	0	91.49	0.719		3.05	1.00	
	1/6	17.10	0.972		0.59	1.00	
	1/2	1.96	1.00		0.06	1.00	
1142.0	0	91.74		155.94	3.94		1.35
	1/6	30.84		179.46	0.83		0.27
	1/2	4.15		1.25	0.10		0.03

TABLE III. Isoscalar phase shifts.

E_c (total c.m. energy) (MeV)	\bar{k} (fm ⁻²)	Full coupling		Without hyperfine			
		δ_1 (deg)	ϵ_1	δ_2 (deg)	δ_1 (deg)	ϵ_1	δ_2 (deg)
1042.0	0	125.92	0.804		6.56	1.00	
	1/6	50.39	0.821		1.18	1.00	
	1/2	4.18	0.998		0.12	1.00	
1142.0	0	112.10		142.78	9.26		4.38
	1/6	86.34		151.52	1.86		0.90
	1/2	9.28		3.83	0.21		0.10

posed in this paper (equivalent to using nonzero values of \bar{k}) implies a decrease in the $K\bar{K}$ coupling. That means that we need to increase the couplings even more so as to get binding. The factors so needed for the different values of \bar{k} are reported in Table I, along with the corresponding energy values for the resulting binding.

In addition to these main results, we report below for completeness (in Tables II and III) the $K\bar{K}$ elastic phase shifts for the three values of \bar{k} , for the center-of-mass energy 50 MeV above the threshold. Moreover, we mention some values of inelastic phase shifts for incoming waves in $K\bar{K}$ and in the second channel (i.e., $\eta\eta$ in the isoscalar and $\pi\eta'$ in the isovector one), along with all these phase shifts in the absence of the hyperfine interaction (without any increase in the remaining coupling). The full interaction phase shifts reported here are for an interaction with the hyperfine part increased by the above mentioned factor of 1.926. With this increase we get bound states of the whole $K\bar{K}$ system for $\bar{k} = 0$ in both the isoscalar and the isovector sectors, and what is explored here is just the effect of our proposed modification to the potential. The numerical procedure to get these phase shifts was based on Eqs. (4.38) and (4.39). Each of them is a complex equation and hence can be solved for the two quantities ϵ_k (the inelasticity factor) and δ_k (the phase shift), with $k = 1$ or 2 , for each value of energy.

However, it must be emphasized that, because of the various approximations which we have used, it would be improper to take these phase shift values as the precise results of our model. One of the indications of this inaccuracy is the violation of unitarity resulting from our separable approximation to the actual nonseparable terms in the coupled equations (4.27) and (4.28). As mentioned in the paragraph following Eq. (4.32), this approximation badly affects our results for the phase shifts, although *not* our main conclusions, i.e., those regarding $K\bar{K}$ binding. For the elastic region this unitarity violation manifests itself in the reported (see Tables II and III) deviation from unity of the inelasticity factor ϵ_1 . Keeping this in mind, the phase shifts reported here are just meant to demonstrate further the appreciable weakening of the interaction because of the gluonic effects, but the only quantitatively significant results of our model for this decrease are those reported in Table I.

VI. CONCLUSIONS

In this paper a lattice-gauge-theory-motivated formalism has been developed to deal with meson-meson sys-

tems with quark-exchange dynamics and applied, as a first application to a realistic case, to $K\bar{K}$ systems. Here we had to increase our resulting coupling by some numerical factor before we could get a bound state of the whole system, even in the two-body potential limit. The variational calculations based on the two-body potential reported in [7] claim to get bound states of the whole $K\bar{K}$ system, concluding that the two scalar meson resonances $f_0(975)$ and $a_0(980)$ can be explained as loosely bound $K\bar{K}$ states in the isoscalar and the isovector sectors, respectively. Our detailed model of meson-meson dynamics, even in the two-body potential model limit, is different to theirs, mainly because of our restricted (i.e., only in the $2S$ diagonal term) incorporation of the annihilation effects. This neglect of the annihilation effects may have appreciably decreased the $K\bar{K}$ binding arising through our model. This is expected because the quark-antiquark annihilation, incorporating the process $K\bar{K} \leftrightarrow \pi\pi$, was [28] a major contribution towards the $K\bar{K}$ binding reported in [7]. Moreover, we might be underestimating the hyperfine interaction by treating this interaction partially as a perturbation, although in our work as well the hyperfine coupling turned out to be the main interaction arising through the quark exchange mechanism. It is difficult to say more about this problem unless a more refined treatment of the hyperfine interaction, along with the annihilation effects, is carried out. On the other hand, the fitting of the model parameters in [7] includes adjusting the ranges and normalization of their effective meson-meson potentials in an *ad hoc* way, and it is not clear how that affects their results.

Leaving these issues to some future work, we looked for any possible change in one of our parameters so as to get $K\bar{K}$ bound states in the $\bar{k} = 0$ limit (where our model would roughly correspond to that used in [7]) and then determined the effects of going beyond that limit, i.e., of using our theoretically improved *four-body* potential. This investigation showed the same trend as observed in the spin-independent case reported in [11]: increasing \bar{k} , i.e., decreasing the gluonic states overlap, results in a significantly weaker meson-meson interaction. This means that, if we get a $K\bar{K}$ bound state in the two-body potential model limit, we do not necessarily get one with our QCD-inspired refinement of the $q^2\bar{q}^2$ potential.

Much improvement in the calculations can be made by going beyond the approximations we have used, giving more precise results. But even without this being carried out, this work clearly indicates that the theoretical refinement of the four-body potential results in an ap-

preciable decrease in a major part of the meson-meson interaction—enough to cast doubt on any result based on a naive two-body potential model.

ACKNOWLEDGMENTS

I would like to express my gratitude to J. Paton for a useful collaboration as a supervisor during my stay in

Oxford, U.K., and for help in writing this paper. Moreover I extend my thanks to A. M. Green for many enlightening discussions, a fruitful collaboration, especially during my stay in Helsinki, and for carefully reading the manuscript. I thank the Oxford Students Scholarship Committee, Oriel College, Oxford, the ICSC World Laboratory, and the University of Helsinki for their financial assistance during different stages of this work. I would also like to thank J. Weinstein for a helpful discussion.

APPENDIX A: THE SPIN BASIS

In the main part of this paper, we use the spin basis given through the Eqs. (3.1), (3.2), and (3.3). The notation used in these equations is that of the Appendix D of [7]. In this notation, an orthonormal spin basis is $|S_{12}S_{34}\rangle_s$ and $|\mathbf{A}_{12} \cdot \mathbf{A}_{34}\rangle_s$, defined through Eqs. (D3) and (D4) there. Our remaining spin base states are given in terms of these by Eqs. (D5)–(D8) of the same. These equations give easily the overlaps of our spin base states, written as ${}_s\langle kI|lJ\rangle_s$ in the results mentioned in Appendix B, as elements of the overlap matrix

$$A = \begin{pmatrix} 1 & 0 & \sqrt{1/4} & -\sqrt{3/4} & \sqrt{1/4} & \sqrt{3/4} \\ & 1 & -\sqrt{3/4} & -\sqrt{1/4} & \sqrt{3/4} & -\sqrt{1/4} \\ & & 1 & 0 & -\sqrt{1/4} & \sqrt{3/4} \\ & & & 1 & -\sqrt{3/4} & -\sqrt{1/4} \\ & & & & 1 & 0 \\ \text{symmetric} & & & & & 1 \end{pmatrix}, \quad (\text{A1})$$

in the basis $|1S\rangle_s, |1T\rangle_s, \dots, |3T\rangle_s$.

For the matrix elements of the $\mathbf{S}_i \cdot \mathbf{S}_j$ operators, for different values of the indices i and j , in our spin basis, we also used the results expressed through Eqs. (D9)–(D11) of the Appendix D of [7]. Some of the results obtained in this way are reported here:

$${}_s\langle 1S| \begin{bmatrix} \mathbf{S}_1 \cdot \mathbf{S}_2 \\ \mathbf{S}_1 \cdot \mathbf{S}_3 \\ \mathbf{S}_1 \cdot \mathbf{S}_4 \\ \mathbf{S}_2 \cdot \mathbf{S}_3 \\ \mathbf{S}_2 \cdot \mathbf{S}_4 \\ \mathbf{S}_3 \cdot \mathbf{S}_4 \end{bmatrix} |1S\rangle_s = {}_s\langle P_{13}P_{24}| \begin{bmatrix} \mathbf{S}_1 \cdot \mathbf{S}_2 \\ \mathbf{S}_1 \cdot \mathbf{S}_3 \\ \mathbf{S}_1 \cdot \mathbf{S}_4 \\ \mathbf{S}_2 \cdot \mathbf{S}_3 \\ \mathbf{S}_2 \cdot \mathbf{S}_4 \\ \mathbf{S}_3 \cdot \mathbf{S}_4 \end{bmatrix} |P_{13}P_{24}\rangle_s = \begin{bmatrix} 0 \\ -\frac{3}{4} \\ 0 \\ 0 \\ -\frac{3}{4} \\ 0 \end{bmatrix}, \quad (\text{A2})$$

$${}_s\langle 1S| \begin{bmatrix} \mathbf{S}_1 \cdot \mathbf{S}_2 \\ \mathbf{S}_1 \cdot \mathbf{S}_3 \\ \mathbf{S}_1 \cdot \mathbf{S}_4 \\ \mathbf{S}_2 \cdot \mathbf{S}_3 \\ \mathbf{S}_2 \cdot \mathbf{S}_4 \\ \mathbf{S}_3 \cdot \mathbf{S}_4 \end{bmatrix} |1T\rangle_s = {}_s\langle 1T| \begin{bmatrix} \mathbf{S}_1 \cdot \mathbf{S}_2 \\ \mathbf{S}_1 \cdot \mathbf{S}_3 \\ \mathbf{S}_1 \cdot \mathbf{S}_4 \\ \mathbf{S}_2 \cdot \mathbf{S}_3 \\ \mathbf{S}_2 \cdot \mathbf{S}_4 \\ \mathbf{S}_3 \cdot \mathbf{S}_4 \end{bmatrix} |1S\rangle_s = \begin{bmatrix} -\sqrt{\frac{3}{16}} \\ 0 \\ +\sqrt{\frac{3}{16}} \\ +\sqrt{\frac{3}{16}} \\ 0 \\ -\sqrt{\frac{3}{16}} \end{bmatrix}, \quad (\text{A3})$$

$${}_s\langle 1T| \begin{bmatrix} \mathbf{S}_1 \cdot \mathbf{S}_2 \\ \mathbf{S}_1 \cdot \mathbf{S}_3 \\ \mathbf{S}_1 \cdot \mathbf{S}_4 \\ \mathbf{S}_2 \cdot \mathbf{S}_3 \\ \mathbf{S}_2 \cdot \mathbf{S}_4 \\ \mathbf{S}_3 \cdot \mathbf{S}_4 \end{bmatrix} |1T\rangle_s = {}_s\langle \mathbf{V}_{13} \cdot \mathbf{V}_{24}| \begin{bmatrix} \mathbf{S}_1 \cdot \mathbf{S}_2 \\ \mathbf{S}_1 \cdot \mathbf{S}_3 \\ \mathbf{S}_1 \cdot \mathbf{S}_4 \\ \mathbf{S}_2 \cdot \mathbf{S}_3 \\ \mathbf{S}_2 \cdot \mathbf{S}_4 \\ \mathbf{S}_3 \cdot \mathbf{S}_4 \end{bmatrix} |\mathbf{V}_{13} \cdot \mathbf{V}_{24}\rangle_s = \begin{bmatrix} -\frac{1}{2} \\ +\frac{1}{4} \\ -\frac{1}{2} \\ -\frac{1}{2} \\ +\frac{1}{4} \\ -\frac{1}{2} \end{bmatrix}, \quad (\text{A4})$$

$${}_s\langle 1S| \begin{bmatrix} \mathbf{S}_1 \cdot \mathbf{S}_2 \\ \mathbf{S}_1 \cdot \mathbf{S}_3 \\ \mathbf{S}_1 \cdot \mathbf{S}_4 \\ \mathbf{S}_2 \cdot \mathbf{S}_3 \\ \mathbf{S}_2 \cdot \mathbf{S}_4 \\ \mathbf{S}_3 \cdot \mathbf{S}_4 \end{bmatrix} |2S\rangle_s = {}_s\langle 2S| \begin{bmatrix} \mathbf{S}_1 \cdot \mathbf{S}_2 \\ \mathbf{S}_1 \cdot \mathbf{S}_3 \\ \mathbf{S}_1 \cdot \mathbf{S}_4 \\ \mathbf{S}_2 \cdot \mathbf{S}_3 \\ \mathbf{S}_2 \cdot \mathbf{S}_4 \\ \mathbf{S}_3 \cdot \mathbf{S}_4 \end{bmatrix} |1S\rangle_s = \begin{bmatrix} +\frac{3}{8} \\ -\frac{3}{8} \\ -\frac{3}{8} \\ -\frac{3}{8} \\ -\frac{3}{8} \\ +\frac{3}{8} \end{bmatrix}, \quad (\text{A5})$$

$${}_s\langle 2S | \begin{bmatrix} \mathbf{S}_1 \cdot \mathbf{S}_2 \\ \mathbf{S}_1 \cdot \mathbf{S}_3 \\ \mathbf{S}_1 \cdot \mathbf{S}_4 \\ \mathbf{S}_2 \cdot \mathbf{S}_3 \\ \mathbf{S}_2 \cdot \mathbf{S}_4 \\ \mathbf{S}_3 \cdot \mathbf{S}_4 \end{bmatrix} | 2S \rangle_s = {}_s\langle P_{1\bar{4}} P_{2\bar{3}} | \begin{bmatrix} \mathbf{S}_1 \cdot \mathbf{S}_2 \\ \mathbf{S}_1 \cdot \mathbf{S}_3 \\ \mathbf{S}_1 \cdot \mathbf{S}_4 \\ \mathbf{S}_2 \cdot \mathbf{S}_3 \\ \mathbf{S}_2 \cdot \mathbf{S}_4 \\ \mathbf{S}_3 \cdot \mathbf{S}_4 \end{bmatrix} | P_{1\bar{4}} P_{2\bar{3}} \rangle_s = \begin{bmatrix} 0 \\ 0 \\ -\frac{3}{4} \\ -\frac{3}{4} \\ 0 \\ 0 \end{bmatrix}. \tag{A6}$$

APPENDIX B: THE KERNELS OF THE INTEGRODIFFERENTIAL EQUATIONS

The results for (in general, nonlocal) kernels appearing in Eq. (4.19), calculated using the procedure outlined in the two paragraphs following this equation, are

$$\mathcal{N}_{kI,kJ} = \delta_{IJ} \delta(\mathbf{R}_k - \mathbf{R}'_k) \tag{B1}$$

for all values of $k, I,$ and J and

$$\mathcal{K}_{kI,kJ} = \delta_{IJ} \delta(\mathbf{R}_k - \mathbf{R}'_k) \left[\frac{3}{4} [\omega_{k1} + \omega_{k2}] - \frac{f_k}{2m} \nabla_{\mathbf{R}_k}^2 \right], \tag{B2}$$

for all values of $k, I,$ and $J,$ except those corresponding to the $2S$ diagonal term. Here

$$\omega_{k1} = \frac{g_k}{2md_{k1}^2} \quad \text{and} \quad \omega_{k2} = \frac{h_k}{2md_{k2}^2}, \tag{B3}$$

along with

$$\begin{aligned} f_1 = f_3 &= \frac{2}{s+1}, \\ g_1 = g_3 = h_1 = h_3 &= \frac{s+1}{s}, \\ f_2 &= \frac{s+1}{2s}, \\ g_2 &= 2, \\ h_2 &= \frac{2}{s}. \end{aligned} \tag{B4}$$

d_{k1} and $d_{k2},$ for $k = 1, 2,$ or $3,$ are the same ones which appear in Eq. (4.6):

$$\mathcal{V}_{1I,1J}^{\text{cf}} = \delta_{IJ} \delta(\mathbf{R}_1 - \mathbf{R}'_1) \left(-\frac{8}{3} \bar{C} - 4C[d_{11}^2 + d_{12}^2] \right), \tag{B5}$$

for $I, J = S$ or $T.$ Similarly,

$$\mathcal{V}_{2I,2J}^{\text{cf}} = \delta_{IJ} \delta(\mathbf{R}_2 - \mathbf{R}'_2) \left(-\frac{8}{3} \bar{C} - 4C[d_{21}^2 + d_{22}^2] \right), \tag{B6}$$

$$\mathcal{V}_{3I,3J}^{\text{cf}} = \delta_{IJ} \delta(\mathbf{R}_3 - \mathbf{R}'_3)$$

$$\begin{aligned} &\times \left\{ -\frac{8}{3} \bar{C} - \frac{4}{3} C \mathbf{R}_3^2 - 6C d'^2 - 2C d'^2 \left(\frac{s-1}{s+1} \right)^2 \right. \\ &+ \frac{5}{2} \frac{D}{(1+4\bar{k}d'^2)^{3/2}} \frac{[s+1]^3}{[8\bar{k}d'^2(s^2+1) + (s+1)^2]^{3/2}} \\ &\times \exp \left[4\bar{k}(s-1)^2 \mathbf{R}_3^2 \left(\frac{4\bar{k}d'^2}{8\bar{k}d'^2(s^2+1) + (s+1)^2} - \frac{1}{(s-1)^2} \right) \right] \\ &- \frac{5}{2} \frac{D}{(1+8\bar{k}d'^2)^{3/2}} \frac{[s+1]^3}{[16\bar{k}d'^2(s^2+1) + (s+1)^2]^{3/2}} \\ &\left. \times \exp \left[8\bar{k}(s-1)^2 \mathbf{R}_3^2 \left(\frac{8\bar{k}d'^2}{16\bar{k}d'^2(s^2+1) + (s+1)^2} - \frac{1}{(s-1)^2} \right) \right] \right\} \end{aligned} \tag{B7}$$

[see the discussion before Eq. (4.7) for $d',$

$$\mathcal{V}_{1S,1S}^{\text{hyp}} = -\frac{8\pi}{3m^2 s} \delta(\mathbf{R}_1 - \mathbf{R}'_1) \left[\frac{\alpha_s^{13}}{(2\pi d_{11}^2)^{3/2}} + \frac{\alpha_s^{24}}{(2\pi d_{12}^2)^{3/2}} \right], \tag{B8}$$

$$\mathcal{V}_{1T,1T}^{\text{hyp}} = -\frac{1}{3} \mathcal{V}_{1S,1S}^{\text{hyp}}, \tag{B9}$$

$$\mathcal{V}_{2T,2T}^{\text{hyp}} = \frac{1}{3} \frac{8\pi}{3m^2 s} \delta(\mathbf{R}_2 - \mathbf{R}'_2) \left[\frac{s\alpha_s^{14}}{(2\pi d_{21}^2)^{3/2}} + \frac{\alpha_s^{23}}{s(2\pi d_{22}^2)^{3/2}} \right], \tag{B10}$$

$$\mathcal{V}_{3S,3S}^{\text{hyp}} = -\frac{1}{2} \frac{8\pi}{3m^2 s} \delta(\mathbf{R}_3 - \mathbf{R}'_3) \frac{1}{(2\pi d'^2)^{3/2}} \left[\alpha_s^{12} + \alpha_s^{34} \right], \tag{B11}$$

$$\mathcal{V}_{3S,3T}^{\text{hyp}} = \mathcal{V}_{3T,3S}^{\text{hyp}} = -\frac{1}{4\sqrt{3}} \frac{8\pi}{3m_s^2} \delta(\mathbf{R}_3 - \mathbf{R}'_3) \frac{1}{(2\pi d'^2)^{3/2}} \left\{ \left[\alpha_s^{13} + \alpha_s^{2\bar{4}} \right] \left[\frac{(s+1)^2}{(s^2+1)} \right]^{3/2} \exp \left[-\frac{\mathbf{R}_3^2 (s+1)^2}{2d'^2 (s^2+1)} \right] \right. \\ \left. - s\alpha_s^{1\bar{4}} \left[\frac{(s+1)^2}{2s^2} \right]^{3/2} \exp \left[-\frac{\mathbf{R}_3^2 (s+1)^2}{2d'^2 2s^2} \right] - \frac{\alpha_s^{2\bar{3}}}{s} \left[\frac{(s+1)^2}{2} \right]^{3/2} \exp \left[-\frac{\mathbf{R}_3^2 (s+1)^2}{2d'^2 2} \right] \right\}, \quad (\text{B12})$$

$$\mathcal{V}_{3T,3T}^{\text{hyp}} = -\frac{1}{6} \frac{8\pi}{3m_s^2} \delta(\mathbf{R}_3 - \mathbf{R}'_3) \frac{1}{(2\pi d'^2)^{3/2}} \\ \times \left\{ - \left[\alpha_s^{12} + \alpha_s^{3\bar{4}} \right] + \left[\alpha_s^{13} + \alpha_s^{2\bar{4}} \right] \left[\frac{(s+1)^2}{(s^2+1)} \right]^{3/2} \exp \left[-\frac{\mathbf{R}_3^2 (s+1)^2}{2d'^2 (s^2+1)} \right] \right. \\ \left. + s\alpha_s^{1\bar{4}} \left[\frac{(s+1)^2}{2s^2} \right]^{3/2} \exp \left[-\frac{\mathbf{R}_3^2 (s+1)^2}{2d'^2 2s^2} \right] + \frac{\alpha_s^{2\bar{3}}}{s} \left[\frac{(s+1)^2}{2} \right]^{3/2} \exp \left[-\frac{\mathbf{R}_3^2 (s+1)^2}{2d'^2 2} \right] \right\}. \quad (\text{B13})$$

$$\mathcal{N}_{kI,2J} = e_0 \langle kI|2J \rangle_s N_{k,2}^0 \exp[-e_1 \mathbf{R}_k^2 - e_2 \mathbf{R}_2^2] \quad \text{for } k=1 \text{ or } 3, \quad (\text{B14})$$

$$\mathcal{N}_{2I,lJ} = e_0 \langle 2I|lJ \rangle_s N_{2,l}^0 \exp[-e_1 \mathbf{R}_l^2 - e_2 \mathbf{R}_2^2] \quad \text{for } l=1 \text{ or } 3, \quad (\text{B15})$$

$$\mathcal{N}_{kI,lJ} = \langle kI|lJ \rangle_s N_{k,l}^0 \frac{(s+1)^6}{64s^3} \left[\frac{1}{\pi d'^2 (1+4\bar{k}d'^2)} \right]^{3/2} \\ \times \exp \left\{ - \left(\frac{s+1}{2} \right)^2 \left(\frac{1+8\bar{k}d'^2}{4d'^2} \right) \left[\frac{s^2+1}{s^2} (\mathbf{R}_k^2 + \mathbf{R}_l^2) + 2 \frac{s^2-1}{s^2} \mathbf{R}_k \cdot \mathbf{R}_l \right] \right\} \quad \text{for } k, l=1 \text{ or } 3, \quad (\text{B16})$$

but with $k \neq l$. Here,

$$e_0 = (s+1)^{9/4} s^{-15/8} 2^{3/4} (\pi \kappa d^2)^{-3/2}, \quad (\text{B17})$$

$$e_1 = \frac{1}{4d^2} \left(\frac{s+1}{2} \right)^2 \left[\gamma - \frac{\lambda^2}{\kappa} \right], \quad (\text{B18})$$

$$e_2 = 4\bar{k} + \frac{1}{2d^2} \sqrt{\frac{2s}{s+1}}, \quad (\text{B19})$$

with

$$\kappa = 8\bar{k}d^2 \left[\frac{s^2+1}{s^2} \right] + 1 + s^{-3/2} \left[\frac{(s+1)^2}{\sqrt{2(s+1)}} + 1 \right], \quad (\text{B20})$$

$$\lambda = 8\bar{k}d^2 \left[\frac{s^2-1}{s^2} \right] + 1 + s^{-3/2} \left[\frac{s^2-1}{\sqrt{2(s+1)}} - 1 \right], \quad (\text{B21})$$

$$\gamma = 8\bar{k}d^2 \left[\frac{s^2+1}{s^2} \right] + 1 + s^{-3/2} \left[\frac{(s-1)^2}{\sqrt{2(s+1)}} + 1 \right]. \quad (\text{B22})$$

$$\mathcal{K}_{kI,2J} = -\frac{e_0}{2m_s} \langle kI|2J \rangle_s N_{k,2}^0 [q_{11} \mathbf{R}_k^2 + q_{12} \mathbf{R}_2^2 + q_{10}] \exp[-e_1 \mathbf{R}_k^2 - e_2 \mathbf{R}_2^2] \quad \text{for } k=1 \text{ or } 3, \quad (\text{B23})$$

$$\mathcal{K}_{2I,lJ} = -\frac{e_0}{2m_s} \langle 2I|lJ \rangle_s N_{2,l}^0 [q_{21} \mathbf{R}_l^2 + q_{22} \mathbf{R}_2^2 + q_{20}] \exp[-e_1 \mathbf{R}_l^2 - e_2 \mathbf{R}_2^2] \quad \text{for } l=1 \text{ or } 3, \quad (\text{B24})$$

$$\mathcal{K}_{kI,lJ} = -\frac{1}{2m_s} \langle kI|lJ \rangle_s N_{k,l}^0 \frac{(s+1)^6}{64s^3} \left[\frac{1}{\pi d'^2 (1+4\bar{k}d'^2)} \right]^{3/2} \\ \times \left\{ \left(\frac{s+1}{2} \right)^4 \left[\left(\frac{s-1}{s+1} \right)^2 \mathbf{R}_k^2 \left(\frac{8(s-1)^2}{(s+1)^3} \left[\frac{4}{(s-1)^2} + \frac{1}{s} \right]^2 \left[\frac{1+4\bar{k}d'^2}{2d'^2} \right]^2 + \frac{32s}{(s+1)^3} \frac{(s+1)^4}{s^4} \left[\frac{1+8\bar{k}d'^2}{8d'^2} \right]^2 \right) \right. \right. \\ \left. - 2 \left(\frac{s-1}{s+1} \right) \mathbf{R}_k \cdot \mathbf{R}_l \left(\frac{8(s-1)^2}{(s+1)^3} \frac{1}{s} \left[\frac{4}{(s-1)^2} + \frac{1}{s} \right] \left[\frac{1+4\bar{k}d'^2}{2d'^2} \right]^2 \right. \right. \\ \left. \left. + \frac{32s}{(s+1)^3} \frac{(s+1)^2}{s^2} \left[\frac{1+8\bar{k}d'^2}{8d'^2} \right] \frac{1}{s^2} \left[\frac{(s+1)^2 + (1+s^2)8\bar{k}d'^2}{8d'^2} \right] \right) \right. \\ \left. \left. + \mathbf{R}_l^2 \left(\frac{8(s-1)^2}{(s+1)^3} \frac{1}{s^2} \left[\frac{1+4\bar{k}d'^2}{2d'^2} \right]^2 + \frac{32s}{(s+1)^3} \frac{1}{s^4} \left[\frac{(s+1)^2 + (1+s^2)8\bar{k}d'^2}{8d'^2} \right]^2 \right) \right\} \right]$$

$$\begin{aligned}
& -6 \left(\frac{s+1}{4} \right)^2 \left[\frac{8(s-1)^2}{(s+1)^3} \frac{4}{(s-1)^2} \left(\frac{1+4\bar{k}d'^2}{2d'^2} \right) \right. \\
& \left. + \frac{32s}{(s+1)^3} \frac{1}{s^2} \left(\frac{(s+1)^2 + (1+s^2)8\bar{k}d'^2}{8d'^2} \right) \right] - 3 \left(\frac{s+1}{2s} \right) \left[\frac{1+4\bar{k}d'^2}{2d'^2} \right] \\
& \times \exp \left\{ - \left(\frac{s+1}{2} \right)^2 \left(\frac{1+8\bar{k}d'^2}{4d'^2} \right) \left[\frac{s^2+1}{s^2} (\mathbf{R}_k^2 + \mathbf{R}_l^2) + 2 \frac{s^2-1}{s^2} \mathbf{R}_k \cdot \mathbf{R}_l \right] \right\}
\end{aligned}$$

for $k, l = 1$ or 3 , (B25)

but with $k \neq l$. Here,

$$\begin{aligned}
q_{11} = & \left(\frac{s+1}{2} \right)^4 \left\{ \frac{8(s-1)^2}{(s+1)^3} \left[\left(\frac{s-1}{s+1} \right) \left(\frac{8\bar{k}}{(s-1)^2} + \frac{1+\sqrt{s}}{(s-1)^2 d^2} \right) - \left(\frac{\lambda}{\kappa} - \frac{s-1}{s+1} \right) \left(\frac{2\bar{k}}{s} + \frac{1}{2d^2 \sqrt{s}(1+\sqrt{s})} \right) \right] \right. \\
& \left. + \frac{32s}{(s+1)^3} \left[\left(\frac{s-1}{s+1} \right) \left(\frac{2\bar{k}}{s} + \frac{1}{2d^2 \sqrt{s}(1+\sqrt{s})} \right) - \left(\frac{\lambda}{\kappa} - \frac{s-1}{s+1} \right) \left(\bar{k} \frac{s^2+1}{s^2} + \frac{s^{-3/2}+1}{4d^2} \right) \right] \right\}^2, \quad (\text{B26})
\end{aligned}$$

$$q_{12} = 4 \left(\frac{s+1}{2s} \right) \left[2\bar{k} + \frac{1}{2d^2} \sqrt{\frac{2s}{s+1}} \right]^2, \quad (\text{B27})$$

$$\begin{aligned}
q_{10} = & -\frac{3}{2} \left(\frac{s+1}{2} \right)^2 \left[\frac{8(s-1)^2}{(s+1)^3} \left(\frac{8\bar{k}}{(s-1)^2} + \frac{1+\sqrt{s}}{(s-1)^2 d^2} \right) + \frac{32s}{(s+1)^3} \left(\bar{k} \frac{s^2+1}{s^2} + \frac{s^{-3/2}+1}{4d^2} \right) \right] \\
& + \frac{3d^2}{2\kappa} (s+1)^2 \left[\frac{8(s-1)^2}{(s+1)^3} \left(\frac{2\bar{k}}{s} + \frac{1}{2d^2 \sqrt{s}(1+\sqrt{s})} \right)^2 + \frac{32s}{(s+1)^3} \left(\bar{k} \frac{s^2+1}{s^2} + \frac{s^{-3/2}+1}{4d^2} \right)^2 \right] \\
& - 6 \left(\frac{s+1}{2s} \right) \left[2\bar{k} + \frac{1}{2d^2} \sqrt{\frac{2s}{s+1}} \right], \quad (\text{B28})
\end{aligned}$$

$$q_{21} = 2(s+1)^2 \left[\left(1 - \frac{\lambda}{\kappa} \right)^2 \left(\bar{k} + \frac{1}{4d^2} \right)^2 + s \left(1 + \frac{\lambda}{\kappa} \right)^2 \left(\frac{\bar{k}}{s^2} + \frac{s^{-3/2}}{4d^2} \right)^2 \right], \quad (\text{B29})$$

$$q_{22} = 4 \left(\frac{s+1}{2s} \right) \left[2\bar{k} + \frac{1}{2d^2} \sqrt{\frac{2s}{s+1}} \right]^2, \quad (\text{B30})$$

$$\begin{aligned}
q_{20} = & \frac{8}{(s+1)^2} \left(\frac{s+1}{2} \right)^2 \frac{24d^2}{\kappa} \left[\left(\bar{k} + \frac{1}{4d^2} \right)^2 + s \left(\frac{\bar{k}}{s^2} + \frac{s^{-3/2}}{4d^2} \right)^2 \right] \\
& - 6 \times \frac{8}{(s+1)^2} \left(\frac{s+1}{2} \right)^2 \left[\left(\bar{k} + \frac{1}{4d^2} \right) + s \left(\frac{\bar{k}}{s^2} + \frac{s^{-3/2}}{4d^2} \right) \right] - 6 \left(\frac{s+1}{2s} \right) \left[2\bar{k} + \frac{1}{2d^2} \sqrt{\frac{2s}{s+1}} \right]. \quad (\text{B31})
\end{aligned}$$

$$\mathcal{V}_{kI,lJ}^{\text{cf}} = -\frac{8}{3} \bar{C} \mathcal{N}_{kI,lJ} + s \langle kI|lJ \rangle_s \mathcal{V}_{k,l}^{\text{cf}}, \quad (\text{B32})$$

with

$$\mathcal{V}_{1,2}^{\text{cf}} = \mathcal{V}_{2,1}^{\text{cf}} = e_0 [b_1 \mathbf{R}_1^2 + b_0] \exp [-e_1 \mathbf{R}_1^2 - e_2 \mathbf{R}_2^2], \quad (\text{B33})$$

$$\begin{aligned}
\mathcal{V}_{2,3}^{\text{cf}} = \mathcal{V}_{3,2}^{\text{cf}} = & \frac{2}{3\sqrt{3}} C e_0 \frac{(s+1)^2}{2s^2} \left\{ \left[(s^2+s+1) \frac{\lambda^2}{\kappa^2} - 2(s^2-1) \frac{\lambda}{\kappa} + (s^2-s+1) \right] \mathbf{R}_3^2 \right. \\
& \left. + \frac{(s^2+s+1) 24d^2}{(s+1)^2 \kappa} \right\} \exp [-e_1 \mathbf{R}_3^2 - e_2 \mathbf{R}_2^2], \quad (\text{B34})
\end{aligned}$$

$$\begin{aligned}
\mathcal{V}_{1,3}^{\text{cf}} = \mathcal{V}_{3,1}^{\text{cf}} = & -\frac{2}{3\sqrt{3}} C \frac{(s+1)^6}{64s^3} \left[\frac{1}{\pi d'^2 (1+4\bar{k}d'^2)} \right]^{3/2} \left\{ \frac{1}{2s^2} \left(\frac{s+1}{2} \right)^2 [(s+1)\mathbf{R}_3 + (s-1)\mathbf{R}_1]^2 + \frac{9d'^2}{1+4\bar{k}d'^2} \right\} \\
& \times \exp \left\{ - \left(\frac{s+1}{2} \right)^2 \left(\frac{1+8\bar{k}d'^2}{4d'^2} \right) \left[\frac{s^2+1}{s^2} (\mathbf{R}_1^2 + \mathbf{R}_3^2) + 2 \frac{s^2-1}{s^2} \mathbf{R}_1 \cdot \mathbf{R}_3 \right] \right\}. \quad (\text{B35})
\end{aligned}$$

Here the new definitions used are

$$b_1 = -\frac{4}{9}C \frac{(s+1)^4}{4s^2} \left[\frac{\lambda}{\kappa} - \frac{s-1}{s+1} \right]^2, \quad (\text{B36})$$

$$b_0 = -\frac{8}{3}C \left(\frac{s+1}{s} \right)^2 \frac{d^2}{\kappa}. \quad (\text{B37})$$

$$\mathcal{V}_{1S,2S}^{\text{hyp}} = \mathcal{V}_{2S,1S}^{\text{hyp}} = -\frac{e_0}{6} \frac{8\pi}{3m^2s} \frac{(2\kappa)^{3/2}}{(2\pi d^2)^{3/2}} [L_{11} + L_{12} + L_{13}] \exp[-(e_1 + e'_1)\mathbf{R}_1^2 - e_2\mathbf{R}_2^2], \quad (\text{B38})$$

$$\mathcal{V}_{1S,2T}^{\text{hyp}} = \mathcal{V}_{2T,1S}^{\text{hyp}} = -\frac{e_0}{6\sqrt{3}} \frac{8\pi}{3m^2s} \frac{(2\kappa)^{3/2}}{(2\pi d^2)^{3/2}} [-3L_{11} + L_{12} + L_{13}] \exp[-(e_1 + e'_1)\mathbf{R}_1^2 - e_2\mathbf{R}_2^2], \quad (\text{B39})$$

$$\mathcal{V}_{1T,2S}^{\text{hyp}} = \mathcal{V}_{2S,1T}^{\text{hyp}} = -\frac{e_0}{6\sqrt{3}} \frac{8\pi}{3m^2s} \frac{(2\kappa)^{3/2}}{(2\pi d^2)^{3/2}} [L_{11} - 3L_{12} + L_{13}] \exp[-(e_1 + e'_1)\mathbf{R}_1^2 - e_2\mathbf{R}_2^2], \quad (\text{B40})$$

$$\mathcal{V}_{1T,2T}^{\text{hyp}} = \mathcal{V}_{2T,1T}^{\text{hyp}} = -\frac{e_0}{18} \frac{8\pi}{3m^2s} \frac{(2\kappa)^{3/2}}{(2\pi d^2)^{3/2}} [L_{11} + L_{12} + 5L_{13}] \exp[-(e_1 + e'_1)\mathbf{R}_1^2 - e_2\mathbf{R}_2^2], \quad (\text{B41})$$

$$\mathcal{V}_{3S,2S}^{\text{hyp}} = \mathcal{V}_{2S,3S}^{\text{hyp}} = -\frac{e_0}{4\sqrt{3}} \frac{8\pi}{3m^2s} \frac{(2\kappa)^{3/2}}{(2\pi d^2)^{3/2}} [L_{21} + 2L_{22} + L_{23}] \exp[-(e_1 + e'_1)\mathbf{R}_3^2 - e_2\mathbf{R}_2^2], \quad (\text{B42})$$

$$\mathcal{V}_{3S,2T}^{\text{hyp}} = \mathcal{V}_{2T,3S}^{\text{hyp}} = -\frac{e_0}{12} \frac{8\pi}{3m^2s} \frac{(2\kappa)^{3/2}}{(2\pi d^2)^{3/2}} [-L_{21} - 2L_{22} + 3L_{23}] \exp[-(e_1 + e'_1)\mathbf{R}_3^2 - e_2\mathbf{R}_2^2], \quad (\text{B43})$$

$$\mathcal{V}_{3T,2S}^{\text{hyp}} = \mathcal{V}_{2S,3T}^{\text{hyp}} = -\frac{e_0}{12} \frac{8\pi}{3m^2s} \frac{(2\kappa)^{3/2}}{(2\pi d^2)^{3/2}} [L_{21} - 6L_{22} + L_{23}] \exp[-(e_1 + e'_1)\mathbf{R}_3^2 - e_2\mathbf{R}_2^2], \quad (\text{B44})$$

$$\mathcal{V}_{3T,2T}^{\text{hyp}} = \mathcal{V}_{2T,3T}^{\text{hyp}} = \frac{e_0}{12\sqrt{3}} \frac{8\pi}{3m^2s} \frac{(2\kappa)^{3/2}}{(2\pi d^2)^{3/2}} [5L_{21} + 2L_{22} + L_{23}] \exp[-(e_1 + e'_1)\mathbf{R}_3^2 - e_2\mathbf{R}_2^2], \quad (\text{B45})$$

$$\mathcal{V}_{1S,3S}^{\text{hyp}} = \mathcal{V}_{3S,1S}^{\text{hyp}} = -\frac{1}{4\sqrt{3}} \frac{8\pi}{3m^2s} \frac{1}{(2\pi d'^2)^{3/2}} \left(\frac{2}{\pi d'^2} \right)^{3/2} \frac{(s+1)^6}{64s^3} [2L_{31} + L_{32} + L_{33}] \\ \times \exp \left\{ -\left(\frac{s+1}{2} \right)^2 \left(\frac{1+8\bar{k}d'^2}{4d'^2} \right) \left[\frac{s^2+1}{s^2} (\mathbf{R}_1^2 + \mathbf{R}_3^2) + 2\frac{s^2-1}{s^2} \mathbf{R}_1 \cdot \mathbf{R}_3 \right] \right\}, \quad (\text{B46})$$

$$\mathcal{V}_{1S,3T}^{\text{hyp}} = \mathcal{V}_{3T,1S}^{\text{hyp}} = -\frac{1}{12} \frac{8\pi}{3m^2s} \frac{1}{(2\pi d'^2)^{3/2}} \left(\frac{2}{\pi d'^2} \right)^{3/2} \frac{(s+1)^6}{64s^3} [6L_{31} - L_{32} - L_{33}] \\ \times \exp \left\{ -\left(\frac{s+1}{2} \right)^2 \left(\frac{1+8\bar{k}d'^2}{4d'^2} \right) \left[\frac{s^2+1}{s^2} (\mathbf{R}_1^2 + \mathbf{R}_3^2) + 2\frac{s^2-1}{s^2} \mathbf{R}_1 \cdot \mathbf{R}_3 \right] \right\}, \quad (\text{B47})$$

$$\mathcal{V}_{1T,3S}^{\text{hyp}} = \mathcal{V}_{3S,1T}^{\text{hyp}} = -\frac{1}{12} \frac{8\pi}{3m^2s} \frac{1}{(2\pi d'^2)^{3/2}} \left(\frac{2}{\pi d'^2} \right)^{3/2} \frac{(s+1)^6}{64s^3} [-2L_{31} - L_{32} + 3L_{33}] \\ \times \exp \left\{ -\left(\frac{s+1}{2} \right)^2 \left(\frac{1+8\bar{k}d'^2}{4d'^2} \right) \left[\frac{s^2+1}{s^2} (\mathbf{R}_1^2 + \mathbf{R}_3^2) + 2\frac{s^2-1}{s^2} \mathbf{R}_1 \cdot \mathbf{R}_3 \right] \right\}, \quad (\text{B48})$$

$$\mathcal{V}_{1T,3T}^{\text{hyp}} = \mathcal{V}_{3T,1T}^{\text{hyp}} = -\frac{1}{12\sqrt{3}} \frac{8\pi}{3m^2s} \frac{1}{(2\pi d'^2)^{3/2}} \left(\frac{2}{\pi d'^2} \right)^{3/2} \frac{(s+1)^6}{64s^3} [2L_{31} + 5L_{32} + L_{33}] \\ \times \exp \left\{ -\left(\frac{s+1}{2} \right)^2 \left(\frac{1+8\bar{k}d'^2}{4d'^2} \right) \left[\frac{s^2+1}{s^2} (\mathbf{R}_1^2 + \mathbf{R}_3^2) + 2\frac{s^2-1}{s^2} \mathbf{R}_1 \cdot \mathbf{R}_3 \right] \right\}. \quad (\text{B49})$$

Here

$$L_{11} = l_{10} \exp [l_{11}\mathbf{R}_1^2 - l_{12}\mathbf{R}_2^2] \{ \alpha_s^{13} \exp [l_{13}\mathbf{R}_1 \cdot \mathbf{R}_2] \\ + \alpha_s^{24} \exp [-l_{13}\mathbf{R}_1 \cdot \mathbf{R}_2] \}, \quad (\text{B50})$$

$$L_{12} = l_{20} \exp [-l_{21}\mathbf{R}_1^2] \left\{ \alpha_s^{14} \exp [l_{22}\mathbf{R}_1^2] \right. \\ \left. + s\alpha_s^{23} \exp [-l_{22}\mathbf{R}_1^2] \right\}, \quad (\text{B51})$$

$$L_{13} = l_{30} \exp [-l_{31}\mathbf{R}_1^2 - l_{32}\mathbf{R}_2^2] \left\{ \alpha_s^{12} \exp [-l_{33}\mathbf{R}_1 \cdot \mathbf{R}_2] \right. \\ \left. + \alpha_s^{34} \exp [l_{33}\mathbf{R}_1 \cdot \mathbf{R}_2] \right\}, \quad (\text{B52})$$

$$L_{21} = l_{30} \exp [-l_{31}\mathbf{R}_3^2 - l_{32}\mathbf{R}_2^2] \left\{ \alpha_s^{13} \exp [-l_{33}\mathbf{R}_3 \cdot \mathbf{R}_2] \right. \\ \left. + \alpha_s^{24} \exp [l_{33}\mathbf{R}_3 \cdot \mathbf{R}_2] \right\}, \quad (\text{B53})$$

$$L_{22} = l_{20} \exp[-l_{21} \mathbf{R}_3^2] \left\{ \alpha_s^{14} \exp[l_{22} \mathbf{R}_3^2] + s \alpha_s^{23} \exp[-l_{22} \mathbf{R}_3^2] \right\}, \quad (\text{B54})$$

$$L_{23} = l_{10} \exp[l_{11} \mathbf{R}_3^2 - l_{12} \mathbf{R}_2^2] \left\{ \alpha_s^{12} \exp[l_{13} \mathbf{R}_3 \cdot \mathbf{R}_2] + \alpha_s^{34} \exp[-l_{13} \mathbf{R}_3 \cdot \mathbf{R}_2] \right\}, \quad (\text{B55})$$

$$L_{31} = \left[\alpha_s^{13} + \alpha_s^{24} \right] \exp \left\{ -\frac{(s+1)^4}{16s^2} \frac{1 + 4\bar{k}d'^2}{d'^2} \times \left[\left(\frac{s-1}{s+1} \right) \mathbf{R}_1 + \mathbf{R}_3 \right]^2 \right\}, \quad (\text{B56})$$

$$L_{32} = \left[\frac{\pi d'^2}{1 + 4\bar{k}d'^2} \right]^{3/2} \left[\frac{2}{s+1} \right] \left\{ s \alpha_s^{14} \delta(\mathbf{R}_1 + \mathbf{R}_3) + \alpha_s^{23} \delta(\mathbf{R}_1 - \mathbf{R}_3) \right\}, \quad (\text{B57})$$

$$L_{33} = \left[\alpha_s^{12} + \alpha_s^{34} \right] \exp \left\{ -\frac{(s+1)^4}{16s^2} \frac{1 + 4\bar{k}d'^2}{d'^2} \times \left[\mathbf{R}_1 + \left(\frac{s-1}{s+1} \right) \mathbf{R}_3 \right]^2 \right\}, \quad (\text{B58})$$

with

$$e'_1 = \frac{1}{4d^2} \left(\frac{s+1}{2} \right)^2 \frac{\lambda^2}{\kappa}, \quad (\text{B59})$$

$$l_{10} = \left(\frac{s}{s+1} \right)^3, \quad (\text{B60})$$

$$l_{11} = \frac{s^2 - 1}{16d^2} \left[2\lambda - \kappa \left(\frac{s-1}{s+1} \right) \right], \quad (\text{B61})$$

$$l_{12} = \frac{\kappa}{d^2} \left(\frac{s}{s+1} \right)^2, \quad (\text{B62})$$

$$l_{13} = \frac{s}{2d^2} \left[\lambda - \kappa \left(\frac{s-1}{s+1} \right) \right], \quad (\text{B63})$$

$$l_{20} = \frac{s}{8}, \quad (\text{B64})$$

$$l_{21} = \frac{\kappa}{4d^2} \left(\frac{s+1}{2} \right)^2, \quad (\text{B65})$$

$$l_{22} = \frac{\lambda}{2d^2} \left(\frac{s+1}{2} \right)^2, \quad (\text{B66})$$

$$l_{30} = \left(\frac{s}{s-1} \right)^3, \quad (\text{B67})$$

$$l_{31} = \frac{1}{4d^2} \left(\frac{s+1}{2} \right)^2 \left(\frac{s+1}{s-1} \right) \left[-2\lambda + \kappa \left(\frac{s+1}{s-1} \right) \right], \quad (\text{B68})$$

$$l_{32} = \frac{\kappa}{d^2} \left(\frac{s}{s-1} \right)^2, \quad (\text{B69})$$

$$l_{33} = \frac{s}{2d^2} \left(\frac{s+1}{s-1} \right) \left[-\lambda + \kappa \left(\frac{s+1}{s-1} \right) \right]. \quad (\text{B70})$$

As mentioned in the text, in the case of the diagonal term corresponding to the $2S$ channel, the expressions depend upon the physical content of this channel. Thus we have

$$\mathcal{N}_{2S,2S} = \delta(\mathbf{R}_2 - \mathbf{R}'_2) \quad (\text{B71})$$

(irrespective of the physical pseudoscalar mesons present),

$$\begin{aligned} \mathcal{K}_{2S,2S}(\eta\eta) &= \delta(\mathbf{R}_2 - \mathbf{R}'_2) \left\{ \frac{3}{4} [(\omega_{21}^l + \omega_{22}^l) \cos^2 \theta + (\omega_{21}^s + \omega_{22}^s) \sin^2 \theta] \right. \\ &\quad \left. - \frac{1}{2m} (f_2^{ll} \cos^4 \theta + 2f_2^{ls} \cos^2 \theta \sin^2 \theta + f_2^{ss} \sin^4 \theta) \underline{\nabla}_{\mathbf{R}_2}^2 \right\}, \end{aligned} \quad (\text{B72})$$

with

$$\omega_{21}^l = \frac{g_2^l}{2md_{21}^2} = \frac{g_2^l}{2md^2}, \quad \omega_{21}^s = \frac{g_2^s}{2md_{22}^2} = \frac{g_2^s}{2md'^2}, \quad (\text{B73})$$

$$\omega_{22}^l = \frac{h_2^l}{2md_{21}^2} = \frac{h_2^l}{2md^2}, \quad \text{and} \quad \omega_{22}^s = \frac{h_2^s}{2md_{22}^2} = \frac{h_2^s}{2md'^2} \quad (\text{B74})$$

[Here

$$\begin{aligned} f_2^{ll} &= 1, & f_2^{ls} &= \frac{1}{2}(1 + 1/s), & f_2^{ss} &= 1/s, \\ g_2^l &= h_2^l = 2, & \text{and} & & g_2^s &= h_2^s = 2/s. \end{aligned} \quad (\text{B75})$$

$$\mathcal{K}_{2S,2S}(\pi\eta) = \delta(\mathbf{R}_2 - \mathbf{R}'_2) \left[\frac{3}{4} [\omega_{21}^l + \omega_{22}^l \cos^2 \theta + \omega_{22}^s \sin^2 \theta] - \frac{1}{2m} (f_2^{ll} \cos^2 \theta + f_2^{ls} \sin^2 \theta) \underline{\nabla}_{\mathbf{R}_2}^2 \right], \quad (\text{B76})$$

$$\mathcal{K}_{2S,2S}(\pi\eta') = \delta(\mathbf{R}_2 - \mathbf{R}'_2) \left[\frac{3}{4} [\omega_{21}^l + \omega_{22}^l \sin^2 \theta + \omega_{22}^s \cos^2 \theta] - \frac{1}{2m} (f_2^{ll} \sin^2 \theta + f_2^{ls} \cos^2 \theta) \underline{\nabla}_{\mathbf{R}_2}^2 \right]. \quad (\text{B77})$$

$$\mathcal{V}_{2S,2S}^{\text{cf}}(\eta\eta) = \delta(\mathbf{R}_2 - \mathbf{R}'_2) \left([-\frac{8}{3}\bar{C} - 2 \times 4C[d_{21}^2 \cos^2 \theta + d_{22}^2 \sin^2 \theta]] \right), \quad (\text{B78})$$

$$\mathcal{V}_{2S,2S}^{\text{cf}}(\pi\eta) = \delta(\mathbf{R}_2 - \mathbf{R}'_2) \left(-\frac{8}{3}\bar{C} - 4C[d_{21}^2 + d_{21}^2 \cos^2 \theta + d_{22}^2 \sin^2 \theta] \right), \quad (\text{B79})$$

$$\mathcal{V}_{2S,2S}^{\text{cf}}(\pi\eta') = \delta(\mathbf{R}_2 - \mathbf{R}'_2) \left(-\frac{8}{3}\bar{C} - 4C[d_{21}^2 + d_{21}^2 \sin^2 \theta + d_{22}^2 \cos^2 \theta] \right). \quad (\text{B80})$$

$$\mathcal{V}_{2S,2S}^{\text{hyp}}(\eta\eta) = -\frac{8\pi}{3m^2s} \delta(\mathbf{R}_2 - \mathbf{R}'_2) \left[\frac{s(\alpha_s^{14(l)} + \alpha_s^{23(l)}) \cos^2 \theta}{(2\pi d_{21}^2)^{3/2}} + \frac{(\alpha_s^{14(s)} + \alpha_s^{23(s)}) \sin^2 \theta}{s(2\pi d_{22}^2)^{3/2}} \right], \quad (\text{B81})$$

$$\mathcal{V}_{2S,2S}^{\text{hyp}}(\pi\eta) = -\frac{8\pi}{3m^2s} \delta(\mathbf{R}_2 - \mathbf{R}'_2) \left[\frac{s\alpha_s^{14(l)}}{(2\pi d_{21}^2)^{3/2}} + \frac{s\alpha_s^{23(l)} \cos^2 \theta}{(2\pi d_{21}^2)^{3/2}} + \frac{\alpha_s^{23(s)} \sin^2 \theta}{s(2\pi d_{22}^2)^{3/2}} \right], \quad (\text{B82})$$

$$\mathcal{V}_{2S,2S}^{\text{hyp}}(\pi\eta') = -\frac{8\pi}{3m^2s} \delta(\mathbf{R}_2 - \mathbf{R}'_2) \left[\frac{s\alpha_s^{14(l)}}{(2\pi d_{21}^2)^{3/2}} + \frac{s\alpha_s^{23(l)} \sin^2 \theta}{(2\pi d_{21}^2)^{3/2}} + \frac{\alpha_s^{23(s)} \cos^2 \theta}{s(2\pi d_{22}^2)^{3/2}} \right]. \quad (\text{B83})$$

$$\mathcal{V}_{2S,2S}^a(\eta\eta) = 2 \times \delta(\mathbf{R}_2 - \mathbf{R}'_2) [2a_l \cos^2 \theta - 2\sqrt{2a_l a_s} \cos \theta \sin \theta + a_s \sin^2 \theta], \quad (\text{B84})$$

$$\mathcal{V}_{2S,2S}^a(\pi\eta) = \delta(\mathbf{R}_2 - \mathbf{R}'_2) [2a_l \cos^2 \theta - 2\sqrt{2a_l a_s} \cos \theta \sin \theta + a_s \sin^2 \theta], \quad (\text{B85})$$

$$\mathcal{V}_{2S,2S}^a(\pi\eta') = \delta(\mathbf{R}_2 - \mathbf{R}'_2) [2a_l \sin^2 \theta + 2\sqrt{2a_l a_s} \cos \theta \sin \theta + a_s \cos^2 \theta]. \quad (\text{B86})$$

APPENDIX C: THE DEFINITIONS USED IN THE MOMENTUM SPACE SOLUTIONS

The following definitions are used in writing the momentum space solutions (4.33) and (4.34) of the coupled equations.

$$\begin{aligned} Q_1^{(1)} &= \left[-\frac{1}{2m} \frac{q_{11}}{6} + \frac{b_1}{2} \right] F_b(p_1, e_1) + \left[-\frac{1}{2m} \frac{q_{10}}{6} + \frac{b_0}{2} - \frac{E'_c}{6} \right] F_a(p_1, e_1) \\ &\quad - H\alpha_s^u l_{20} F_a(p_1, e_1 + e'_1 + l_{21} - l_{22}) - Hs\alpha_s^{ss} l_{20} F_a(p_1, e_1 + e'_1 + l_{21} + l_{22}), \\ Q_2^{(1)} &= -\frac{1}{2m} \frac{q_{12}}{6} F_a(p_1, e_1), \\ Q_3^{(1)} &= -2H\alpha_s^{ls} l_{10} F_a(p_1, e_1 + e'_1 - l_{11}), \\ Q_4^{(1)} &= -\frac{1}{3} H\alpha_s^{ls} l_{10} l_{13}^2 F_b(p_1, e_1 + e'_1 - l_{11}), \\ Q_5^{(1)} &= -Hn_1 \alpha_s^{ls} l_{30} F_a(p_1, \tau_1 e_1 + e'_1 + l_{31} + e_2 + l_{32} - l_{33}), \\ Q_6^{(1)} &= Hn_1 \alpha_s^{ls} l_{30} F_a(p_1, \tau_1 e_1 + e'_1 + l_{31} + e_2 + l_{32} + l_{33}). \end{aligned} \quad (\text{C1})$$

$$\begin{aligned} Q_1^{(2)} &= -\frac{1}{2m} \frac{q_{22}}{6} F_b(p_2, e_2) + \left[-\frac{1}{2m} \frac{q_{20}}{6} + \frac{b_0}{2} - \frac{E'_c}{6} \right] F_a(p_2, e_2), \\ Q_2^{(2)} &= \left[-\frac{1}{2m} \frac{q_{21}}{6} + \frac{b_1}{2} \right] F_a(p_2, e_2), \\ Q_3^{(2)} &= -H\alpha_s^u l_{20} F_a(p_2, e_2), \\ Q_4^{(2)} &= -Hs\alpha_s^{ss} l_{20} F_a(p_2, e_2), \\ Q_5^{(2)} &= -2H\alpha_s^{ls} l_{10} F_a(p_2, e_2 + l_{12}), \\ Q_6^{(2)} &= -\frac{1}{3} H\alpha_s^{ls} l_{10} l_{13}^2 F_b(p_2, e_2 + l_{12}), \\ Q_7^{(2)} &= -Hn_2 \alpha_s^{ls} l_{30} F_a(p_2, \tau_2 e_1 + e'_1 + l_{31} + e_2 + l_{32} - l_{33}), \\ Q_8^{(2)} &= Hn_2 \alpha_s^{ls} l_{30} F_a(p_2, \tau_2 e_1 + e'_1 + l_{31} + e_2 + l_{32} + l_{33}). \end{aligned} \quad (\text{C2})$$

$$E'_c = E_c + \frac{8}{3}\bar{C} - 2m(s+1), \quad (\text{C3})$$

$$A_k(x) = e_0 \int d^3 \mathbf{R}_k \exp[-x\mathbf{R}_k^2] \chi_{kS}(\mathbf{R}_k), \quad (\text{C4})$$

$$B_k(x) = e_0 \int d^3 \mathbf{R}_k \exp[-x\mathbf{R}_k^2] \mathbf{R}_k^2 \chi_{kS}(\mathbf{R}_k), \quad (\text{C5})$$

$$\chi_{kS}(\mathbf{p}_k) = \int \frac{d^3 \mathbf{R}_k}{(2\pi)^{3/2}} \exp[i\mathbf{p}_k \cdot \mathbf{R}_k] \chi_{kS}(\mathbf{R}_k), \quad (\text{C6})$$

for $k = 1, 2$. $F_a(\mathbf{p}_k, x)$ and $F_b(\mathbf{p}_k, x)$ are similar Fourier transforms of $\exp[-x\mathbf{R}_k^2]$ and $\mathbf{R}_k^2 \exp[-x\mathbf{R}_k^2]$, respectively. Moreover,

$$\Delta_1(p_1) = \frac{p_1^2}{2\mu_{K\bar{K}}} + M_K + M_{\bar{K}} - E_c - i\varepsilon, \quad (C7)$$

$$\Delta_2(p_2) = \frac{p_2^2}{2\mu_{ab}} + M_a + M_b - E_c - i\varepsilon, \quad (C8)$$

$$p_c(1) = \sqrt{2\mu_{K\bar{K}}(E_c - M_K - M_{\bar{K}})}, \quad (C9)$$

$$p_c(2) = \sqrt{2\mu_{ab}(E_c - M_a - M_b)}. \quad (C10)$$

APPENDIX D: THE ELEMENTS OF THE T MATRIX

Consistent with our definition of the T matrix [see Eqs. (4.38) and (4.39)], the four elements of the 2×2 T matrix are [these can be read off from Eqs. (4.33) and (4.34)]

$$T_{1,1} = 2\mu_{K\bar{K}} \frac{\pi}{2} p_c(1) \left[Q_1^{(1)} A_2(e_2) + Q_2^{(1)} B_2(e_2) + Q_3^{(1)} A_2(e_2 + l_{12}) + Q_4^{(1)} B_2(e_2 + l_{12}) \right. \\ \left. + Q_5^{(1)} A_2(\tau_1 \overline{e_1 + e'_1 + l_{31} + e_2 + l_{32} - l_{33}}) + Q_6^{(1)} A_2(\tau_1 \overline{e_1 + e'_1 + l_{31} + e_2 + l_{32} + l_{33}}) \right], \quad (D1)$$

$$T_{2,1} = 2\mu_{ab} \frac{\pi}{2} p_c(1) \sqrt{\frac{v_2}{v_1}} \left[Q_1^{(2)} A_1(e_1) + Q_2^{(2)} B_1(e_1) \right. \\ \left. + Q_3^{(2)} A_1(e_1 + e'_1 + l_{21} - l_{22}) + Q_4^{(2)} A_1(e_1 + e'_1 + l_{21} + l_{22}) \right. \\ \left. + Q_5^{(2)} A_1(e_1 + e'_1 - l_{11}) + Q_6^{(2)} B_1(e_1 + e'_1 - l_{11}) \right. \\ \left. + Q_7^{(2)} A_1(\tau_2 \overline{e_1 + e'_1 + l_{31} + e_2 + l_{32} - l_{33}}) + Q_8^{(2)} A_1(\tau_2 \overline{e_1 + e'_1 + l_{31} + e_2 + l_{32} + l_{33}}) \right], \quad (D2)$$

$$T_{2,2} = 2\mu_{ab} \frac{\pi}{2} p_c(2) \left[Q_1^{(2)} A_1(e_1) + Q_2^{(2)} B_1(e_1) + Q_3^{(2)} A_1(e_1 + e'_1 + l_{21} - l_{22}) + Q_4^{(2)} A_1(e_1 + e'_1 + l_{21} + l_{22}) \right. \\ \left. + Q_5^{(2)} A_1(e_1 + e'_1 - l_{11}) + Q_6^{(2)} B_1(e_1 + e'_1 - l_{11}) + Q_7^{(2)} A_1(\tau_2 \overline{e_1 + e'_1 + l_{31} + e_2 + l_{32} - l_{33}}) \right. \\ \left. + Q_8^{(2)} A_1(\tau_2 \overline{e_1 + e'_1 + l_{31} + e_2 + l_{32} + l_{33}}) \right], \quad (D3)$$

$$T_{1,2} = 2\mu_{K\bar{K}} \frac{\pi}{2} p_c(1) \sqrt{\frac{v_1}{v_2}} \left[Q_1^{(1)} A_2(e_2) + Q_2^{(1)} B_2(e_2) + Q_3^{(1)} A_2(e_2 + l_{12}) + Q_4^{(1)} B_2(e_2 + l_{12}) \right. \\ \left. + Q_5^{(1)} A_2(\tau_1 \overline{e_1 + e'_1 + l_{31} + e_2 + l_{32} - l_{33}}) + Q_6^{(1)} A_2(\tau_1 \overline{e_1 + e'_1 + l_{31} + e_2 + l_{32} + l_{33}}) \right], \quad (D4)$$

with p_1 and p_2 in $Q_1^{(1)} \dots Q_8^{(2)}$ [see Eqs. (C1) and (C2)] replaced by $p_c(1)$ and $p_c(2)$, respectively. It was checked numerically that $T_{1,2} = T_{2,1}$, satisfying the requirement of ‘‘reciprocity’’ in an inelastic scattering (see p. 528 of [27]).

-
- [1] M. Bander, Phys. Rep. **75**, 206 (1981).
[2] J. Kogut, Rev. Mod. Phys. **55**, 775 (1983).
[3] A. Chodos, R.L. Jaffe, C.B. Thorne, and V. Weisskopf, Phys. Rev. D **9**, 3471 (1974).
[4] A. Chodos, R.L. Jaffe, C.B. Thorne, and K. Johnson, Phys. Rev. D **10**, 2599 (1974).
[5] S. Godfrey and N. Isgur, Phys. Rev. D **32**, 189 (1985).
[6] J. Weinstein and N. Isgur, Phys. Rev. D **27**, 588 (1983).
[7] J. Weinstein and N. Isgur, Phys. Rev. D **41**, 2236 (1990).
[8] T. Barnes and E.S. Swanson, Phys. Rev. D **46**, 131 (1992).
[9] T. Barnes, S. Capstick, M.D. Kovarik, and E.S. Swanson, Phys. Rev. C **48**, 539 (1993).
[10] O.W. Greenberg and H.J. Lipkin, Nucl. Phys. **A370**, 349 (1981), and references therein.
[11] B. Masud, J. Paton, A.M. Green, and G.Q. Liu, Nucl. Phys. **A528**, 477 (1991).
[12] N. Isgur and J. Paton, Phys. Rev. D **31**, 2910 (1985).
[13] J. Merlin and J. Paton, Phys. Rev. D **36**, 902 (1987).
[14] K. Shimizu, Rep. Prog. Phys. **52**, 1 (1989).
[15] Y. Suzuki and K. Hecht, Phys. Rev. C **27**, 299 (1983).
[16] R.R. Schroeder and H.G. Dosch, Nucl. Phys. **A451**, 666 (1986).
[17] A.M. Green and J. Paton, Nucl. Phys. **A492**, 595 (1989).
[18] A.M. Green and G.Q. Liu, Nucl. Phys. **A500**, 529 (1989).
[19] O. Morimatsu, Nucl. Phys. **A505**, 655 (1989).
[20] C. Alexandrou, T. Karapiperis, and O. Morimatsu, Nucl. Phys. **A518**, 723 (1990).
[21] O. Morimatsu, A.M. Green, and J. Paton, Phys. Lett. B **258**, 257 (1991).
[22] A.M. Green, C. Michael, and J. Paton, Nucl. Phys. **A554**, 701 (1993).

- [23] A.M. Green, C. Michael, J. Paton, and M.E. Sainio, *Int. J. Mod. Phys. E* **2:3**, 479 (1993).
- [24] K. Wildermuth and Y.C. Tang, *Clustering Phenomena in Nuclei*, edited by K. Wildermuth and P. Kramer (Vieweg, Braunschweig, 1977), Vol. 1.
- [25] K. Masutani, *Nucl. Phys.* **A468**, 593 (1987).
- [26] Particle Data Group, K. Hikasa *et al.*, *Phys. Rev. D* **45**, S1 (1992).
- [27] J. Blatt and V. Weisskopf, *Theoretical Nuclear Physics* (Wiley, New York, 1952).
- [28] J. Weinstein (private communication).